

1 **Diverse stem-chondrichthyan oral**
2 **structures and evidence for an**
3 **independently acquired acanthodid**
4 **dentition**

5 Richard P. Dearden¹ and Sam Giles^{2,3*}

6 ¹CR2P, Centre de Recherche en Paléontologie–Paris, Muséum
7 national d’Histoire naturelle, Sorbonne Université, Centre National
8 de la Recherche Scientifique, CP 38, 57 rue Cuvier, F75231 Paris
9 cedex 05, France.

10 ²School of Geography, Earth and Environmental Sciences,
11 University of Birmingham, Birmingham, UK

12 ³Department of Earth Sciences, Natural History Museum,
13 Cromwell Road, London SW7 5BD, UK

14 *Corresponding author

15

16 **Abstract**

17 The teeth of sharks famously form a series of transversely-organised files with
18 conveyor-belt replacement that are borne directly on the jaw cartilages, in
19 contrast to the dermal plate-borne dentition of bony fishes that undergoes
20 site-specific replacement. A major obstacle in understanding how this system
21 evolved is the poorly understood relationships of the earliest chondrichthyans
22 and the profusion of morphologically and terminologically diverse bones,
23 cartilages, splints and whorls that they possess. Here we use tomographic
24 methods to investigate mandibular structures in several early branching
25 ‘acanthodian’-grade stem-chondrichthyans. We show that the dentigerous jaw
26 bones of disparate genera of ischnacanthids are united by a common
27 construction, being growing bones with non-shedding dentition. Mandibular
28 splints, which support the ventro-lateral edge of the Meckel’s cartilage in
29 some taxa, are formed from dermal bone and may be an acanthodid
30 synapomorphy. We demonstrate that the teeth of *Acanthodopsis* are borne
31 directly on the mandibular cartilage and that this taxon is deeply nested within
32 an edentulous radiation, representing an unexpected independent origin of
33 teeth. Many or even all of the range of unusual oral structures may be
34 apomorphic, but they should nonetheless be considered when building
35 hypotheses of tooth and jaw evolution, both in chondrichthyans and more
36 broadly.

37 **Keywords (3-6):** dentitions, early vertebrates, acanthodians,
38 chondrichthyans, tooth evolution, Palaeozoic

39 **1. Introduction**

40 The structure and position of teeth and jaws are amongst the major
41 anatomical distinctions between crown osteichthyans (bony fishes: ray-finned
42 fishes, lobe-finned fishes, and tetrapods) and crown chondrichthyans
43 (cartilaginous fishes: sharks, rays, and chimaeras) [1]. In osteichthyans, teeth
44 are partially resorbed at their base, shed, and replaced in position on dermal
45 bones lateral to and overlying endoskeletal jaw cartilages as part of outer and
46 inner dental arcades. In crownward chondrichthyans, teeth grow, shed, and
47 are replaced in parallel rows of labiolingually-directed series directly on the
48 jaw cartilages. The origins of these dental structures can be traced back to
49 Palaeozoic taxa, which suggest that the last common ancestor of jawed fishes
50 (gnathostomes), as well as crownward stem gnathostomes (a paraphyletic
51 assemblage referred to as ‘placoderms’), possessed non-shedding teeth
52 fused to the underlying dermal jaw bone [2–7]. However, oral structures in
53 many Palaeozoic gnathostomes remain poorly characterised, and as a result
54 their relevance to the evolution of teeth is unclear.

55 The advent of micro-computed tomography has led to a renewed interest in
56 tooth evolution and development in Palaeozoic gnathostomes. These have
57 mostly focussed on stem-gnathostome ‘placoderms’ [2,5,6,8] and
58 osteichthyans [9–14] and have revealed an unexpected range of
59 morphologies. Stem-group gnathostomes have non-shedding dentitions,
60 which may be arranged radially [5,8] or in parallel rows [6], borne on an
61 underlying dermal bone. The homology of the dermal jaw bones in stem-
62 group gnathostomes to the inner and outer dental arcades of crown

63 gnathostomes is uncertain [6,15,16]. Meanwhile, many Palaeozoic
64 osteichthyans possessed shedding dentitions comparable to more recent
65 taxa, although some stem osteichthyans have dental structures such as
66 symphyseal tooth whorls [14] and marginal cusps organised into rows
67 [9,10,11,12,13], which are more broadly comparable in the gnathostome total
68 group. Early-branching members of the chondrichthyan total-group (including
69 ‘acanthodians’), have received less attention, with only a handful of taxa
70 described using CT data [7,17-20]. This is despite a remarkable array of
71 dermal oral structures across the assemblage: various early chondrichthyans
72 possess tooth whorls [17,21,22], gracile or molariform teeth not organised into
73 whorls [18,23,24], dermal plates of differing constrictions with and without
74 teeth [22,23,25-28], or may lack dermal mandibular structures entirely [29]. A
75 variety of extramandibular ‘dentitions’ and other oral structures are also
76 known [29,30].

77 Teeth arranged into files are widespread in chondrichthyans both living and
78 extinct. In the larger of the two constituent chondrichthyan clades
79 (elasmobranchs: sharks and rays), teeth are continuously replaced in
80 generative series [1]. They grow on the inner margin of the jaw, move through
81 a labiolingual file (figure 1a), and are shed at the labial jaw margin [1]. In
82 holocephalans (chimaeras and relatives), the dentition is modified to two
83 upper pairs and one lower pair of non-shedding, hypermineralised toothplates
84 [31]. The elasmobranch-like condition of labiolingual files of teeth is seen in
85 both stem-group elasmobranchs [32] and stem-group holocephalans [33],
86 implying that this condition is plesiomorphic for chondrichthyans. Many
87 Palaeozoic chondrichthyans possessed tooth whorls, where the tooth file

88 comprises multiple cusps fused onto a common base. Tooth whorls are
89 common in taxa in the chondrichthyan stem-group, and may form the entire
90 dentition (e.g. *Ptomacanthus* [21]; *Doliodus* [17]) or be present at and/or
91 restricted to the symphysis (e.g. ischnacanthids: [20,22]). It is unclear whether
92 individual teeth were shed from tooth whorls borne on mandibular rami, or
93 whether the whorls themselves were shed [17]. Some probable crown-group
94 chondrichthyans had a further condition in which teeth did not share a
95 common base but post-functional teeth were retained at the labial margin of
96 the jaw [34]. This, alongside the prevalence of tooth whorls with fused teeth in
97 stem-chondrichthyans, indicates that tooth shedding was acquired later in the
98 chondrichthyan total-group.

99 In addition, a realm of stem-group chondrichthyans have unusual dentitions
100 that do not conform to a file-like arrangement, and which are less commonly
101 considered in hypotheses of tooth evolution (figure 1b-f). The most well-
102 characterised of these are dentigerous jaw bones: large, tooth-bearing dermal
103 plates which sit on both the upper and lower jaw cartilages in 'ischnacanthid'
104 stem-group chondrichthyans [22]. Dentigerous jaw bones bear one or more
105 rows of antero-posteriorly aligned teeth, the cusps of which can be quite
106 morphologically and presumably functionally variable [25]. The tooth rows
107 have been shown to grow via anterior addition of new cusps in one
108 taxonomically unidentified specimen, but construction of the bone beyond the
109 tooth rows, as well as the array of different morphologies, remain poorly
110 characterised [7,26,27]. Other stem-group chondrichthyans, such as
111 *Gladbachus* [24], *Pucapampella* [18] and *Acanthodopsis* [23] have teeth that
112 are neither part of dentigerous jaw bones nor arranged into files. Diplacanthid

113 stem-group chondrichthyans [27,28] bear smooth, toothless dermal plates on
114 their lower jaws. Numerous stem-group chondrichthyans lack teeth altogether,
115 and the lower jaws of many of these taxa bear poorly-characterised
116 mandibular splints [30,37] which have also been identified in some
117 diplacanthids and ischnacanthids [38,39].

118 Further confounding this diversity of oral structures are competing and
119 unsettled hypotheses of relationships for early chondrichthyans. While
120 ‘acanthodians’ are now established as stem-group chondrichthyans [24,32,33,
121 40-44], there is limited certainty over the monophyly of ‘acanthodian’
122 subgroups. There is some evidence that an assemblage of diplacanthiform,
123 ischnacanthiform, and acanthodiform taxa may form a clade or grade
124 subtending the remainder of the chondrichthyan total-group [24]. ‘Climatiid’
125 acanthodians, which have overlapping character complements with more
126 shark-like chondrichthyans [18], tend to be recovered in a more crownward
127 position (although see [35]). Beyond this, however, different phylogenetic
128 analyses present very different schemes of relationships, often with low
129 support. These conflicting patterns of relationships present major obstacles to
130 understanding patterns evolution for many of the dental structures seen in
131 early chondrichthyans, although likelihood-based methods provide a possible
132 approach [7].

133 Here we use computed tomography to image the teeth, jaws and associated
134 oral structures of several early-diverging stem-group chondrichthyans with the
135 aim of more broadly sampling the diversity of their oral structures. We aim to
136 characterise the anatomy of several different ischnacanthid dentigerous jaw
137 bones of different constructions, the mandibular splint of acanthodids, and the

138 'teeth' of *Acanthodopsis*. We contextualise our new data within a wider review
139 of stem-group chondrichthyan oral structures and identify those that represent
140 synapomorphies, while also discussing challenges in reconstructing dental
141 evolutionary histories and homologies.

142

143 **2. Materials and Methods**

144 **2.1 Taxa examined**

145 All specimens studied here are housed at the Natural History Museum,
146 London (NHMUK), and comprise: an isolated jaw of *Taemasacanthus erroli*
147 (NHMUK PV P.33706); an isolated jaw of *Atopacanthus* sp. (NHMUK PV
148 P.10978); an isolated jaw of *Acanthodopsis* sp. (NHMUK PV P.10383); a
149 partial head of *Acanthodes* sp. (NHMUK PV P.8065); and an isolated jaw of
150 *Ischnacanthus* sp. (NHMUK PV P.40124).

151 *Taemasacanthus erroli* is known from eight isolated jaws from the Emsian
152 (Lower Devonian) Murrumbidgee Group in New South Wales, Australia [45].
153 Other species, also based on isolated jaw bones, have been assigned to the
154 genus [46,47], but no articulated animals are known. *Taemasacanthus* is
155 understood to be an ischnacanthid on the basis of its dentigerous jaw bone
156 [45]. NHMUK PV P.33706, described here (figure 2), is a right lower jaw, and
157 comprises two main parts: a dermal dentigerous jaw bone and the articular
158 ossification of Meckel's cartilage. The external morphology of this specimen of
159 *Taemasacanthus* has been fully described [45] but is briefly redescribed here
160 to contextualise our new information. An additional ventral fragment of the

161 articular (previously figured [45]) has become detached from the rest of the
162 ossification and was not included in the CT scan.

163 *Atopacanthus* is known throughout the Middle-Upper Devonian [50]. The type
164 species, *Atopacanthus dentatus*, is known from several dentigerous jaw
165 bones from near Hamburg, New York and is presumed to be an ischnacanthid
166 [23,49]. The sole articulated specimen attributed to *Atopacanthus* sp., from
167 the Upper Devonian of the Rhineland [50,51], has since been referred to
168 *Serradentus* [52] and so the genus is known only from disarticulated remains.

169 The specimen described here, NHMUK PV P.10978 (figure 3), is a
170 dentigerous jaw bone collected from Elgin, Scotland, and is Late Devonian in
171 age. It was originally labelled as a possible dipnoan toothplate before later
172 being referred to *Atopacanthus*, and its morphology conforms with that of
173 other specimens described as *Atopacanthus*. It is not associated with any
174 endoskeletal material, and it is impossible to tell whether it is from a right
175 lower jaw or left upper jaw. For ease of comparison with other specimens, we
176 describe its morphology as if it were a part of the lower jaw.

177 *Ischnacanthus* is the best known ischnacanthid ‘acanthodian’, represented by
178 numerous articulated specimens of Lochkovian (Lower Devonian) age from
179 the Midland Valley in Scotland [22]. The material described here (NHMUK PV
180 P.40124; figure 4) is an isolated left lower jaw from the Lower Devonian
181 (Lochkovian) Midland Valley in Tealing, Forfarshire [53]. It is fairly complete,
182 but parts of the dorsal and anterior margins have been lost to the counterpart
183 (which is preserved, but was not CT scanned), and the whole jaw is laterally
184 flattened. It comprises a dentigerous jaw bone and Meckel’s cartilage.

185 *Acanthodopsis* is known from the Carboniferous of the UK and Australia.
186 *Acanthodopsis* has been previously considered an ischnacanthid on the basis
187 of its “dentigerous jaw bones”, but in terms of its skeletal anatomy it is more
188 similar to acanthodids [23,45]. The material described here, NHMUK PV
189 P.10383 from the Northumberland Coal Measures (figure 5), comprises a
190 laterally flattened lower right jaw, consisting of a Meckel’s cartilage with teeth
191 and a mandibular splint.

192 *Acanthodes* is the latest occurring genus of ‘acanthodian’ found as articulated
193 body fossils from the Mississippian (Carboniferous) into the Lower Permian
194 [31]. It is the only genus of ‘acanthodian’-grade animal known from
195 extensively preserved endoskeleton, seen in specimens of *Acanthodes*
196 *confusus* from Lebach, Germany [54]. The material described here (NHMUK
197 PV P.8065) comprises part of the ventral half of the head of a specimen from
198 the Knowles Ironstone of Staffordshire (figure 6). As the dorsal margins of the
199 jaw bones are obscured within the rock, it was originally referred to
200 ‘*Acanthodopsis* or *Acanthodes*’. As CT scanning shows that dentition is
201 absent, we can confirm it to be *Acanthodes* sp. Most of the left jaw is
202 preserved, and of the right jaw only the mandibular splint is preserved, as are
203 some of the lower branchiostegal ray series and isolated dermal gill rakers.
204 Scattered parts of the rest of the head endoskeleton are also present,
205 including parts of ceratobranchial and a hyomandibular.

206

207 **2.2 CT scanning**

208 Full details of scanning parameters are given in supplementary table 1. The
209 voxel size for each scan are as follows: *Acanthodes*, 44.9 μm ; *Acanthodopsis*,
210 22.6 μm ; *Atopacanthus*, 19.51 μm ; *Ischnacanthus*, 24.6 μm ; *Taemasacanthus*
211 *errol*i, 17.3 μm .

212 Reconstructed tomographic datasets were segmented in Mimics v.19
213 (biomedical.materialise.com/mimics; Materialise, Leuven, Belgium) and
214 images were generated using Blender (blender.org).

215 **2.3 Phylogenetic analyses**

216 Our dataset is based on Dearden *et al.* [44], the most recently published
217 phylogenetic dataset specifically tackling stem-group chondrichthyan
218 relationships. We have added one taxon and four characters and made minor
219 modifications to some codes (full details given in the supplementary text). We
220 performed a parsimony analysis in TNT [55] with the following settings: a
221 parsimony ratchet with 10,000 iterations, holding 100 trees per iteration, with
222 TBR branch swapping. Galeaspida was set as the outgroup and the following
223 constraint applied: (Galeaspida(Osteostraci(Mandibulate Gnathostomes))).
224 We also performed a Bayesian analysis, with Galeaspida set as the outgroup,
225 mandibulate gnathostomes constrained as monophyletic, and the following
226 settings. We used a uniform prior with the Mkv model and gamma-distributed
227 rates; searched for 10,000,000 generations, sampling every 1,000
228 generations; and calculated the majority rule consensus tree with a relative
229 burn-in of 25%.

230

231 **3. Results**

232 **3.1 *Taemasacanthus***

233 The dentigerous jaw bone of *Taemasacanthus* is approximately half the full
234 depth of the jaw and is sinusoidal in dorsal view (figure 2). A circular ridge,
235 previously suggested to be for a labial cartilage attachment [45] but more
236 likely the attachment site for a ligament, is present on the lateral surface
237 approximately $\frac{1}{4}$ of the way along its length (figure 2b,c). Posteriorly, the bone
238 curves laterally and broadens to wrap around the articular. The lateral
239 expansion is larger than the medial expansion, and both are rounded
240 posteriorly. Ventrally, a groove formed by the posterior confluence of these
241 two processes runs underneath the entire length of the dentigerous jaw bone,
242 and would have overlain Meckel's cartilage (figure 2c). The dentigerous jaw
243 bone is approximately trapezoid in cross section, and bears three rows of
244 teeth (figure 2a,b,d,g,h). Histologically the underlying dermal plate comprises
245 heavily vascularised dermal bone, similar to that observed in thin sections of
246 other ischnacanthid dentigerous jaw bones [7,22,56], with a relatively thin
247 layer of less vascularised bone around the plate margins (figure 2g; figure
248 S1a-d). The vascularisation comprises an interlinked network of tubules,
249 which are strongly anteroposteriorly polarised in the tooth-bearing section of
250 the bone. Vascular channels occasionally open onto the surface of the bone,
251 particularly the ventral groove. On the lingual surface of the bone, a change in
252 orientation of the vascularisation (from anteroposterior to more random)
253 indicates the presence of a separate plate-like unit of growth (Figure S1d).
254 The more posterior, wrapped part of the bone has a radial arrangement of
255 vasculature suggesting that the bone grew posteriorly and ventrally as well as
256 anteriorly as the underlying endoskeletal jaw grew. The circular ridge is

257 formed of avascular bone, but is otherwise a similar tissue to that forming the
258 outer margin of the dermal plate (figure 2f).

259 Three rows of teeth are borne on the biting edge of the dermal plate, all
260 starting approximately at the level of the mesial ridge: a lateral, medial, and
261 lingual row (figure 2a,b,d). Teeth of the medial row are far smaller and less
262 distinct than those of the lateral and lingual rows. Teeth within the lateral and
263 lingual rows are fused to the jaw, but the base of the tooth is marked by an
264 increase in the density of random and dorsally-oriented vascular canals
265 (figure 2f; figure S1a-c). The medial row lies on the mesial ridge and
266 comprises a single row of small disorganised cusps that are continuous with
267 the underlying dermal plate and do not appear to overlap with each other.
268 Vasculature in the medial row is only visible in the more posterior cusps and
269 does not seem related to size (figure S1f). The lateral and lingual rows of
270 teeth are much larger and ridged, with a vascular base topped with a mostly
271 avascular crown. The younger, larger, more anterior teeth of both rows have
272 extensively vascularised crowns. The smaller, more posterior cusps have
273 less—or even no—vascularisation, indicating that the crown was infilled in
274 older teeth. The basal vasculature has occasional connections with the
275 vasculature of the underlying dermal plate. The teeth seemingly lack a
276 continuous enameloid covering (figure 2f), contra recent reports of enameloid
277 in an ischnacanthid [7], although we caution that this may be due to the
278 resolution of our dataset. Both tooth rows grow by the addition of new teeth
279 onto the anterior end of the row, as evidenced by anterior teeth partially
280 overlying posterior ones, and cusps becoming progressively larger in the
281 direction of growth. The sole exception to this is in the lingual tooth row,

282 where, in what is probably a pathology, the eighth cusp of the lingual row is
283 incomplete and is either damaged or its growth has been aborted (figure 2a).
284 Both the damaged eighth cusp and the undamaged tenth cusp are overgrown
285 by the youngest cusp in the row. This, the ninth cusp, is oriented noticeably
286 more medially than other cusps and may have disrupted the growth of the
287 smaller tenth cusp, although the underlying bone appears unaffected. The
288 vasculature of the ninth cusp appears to be isolated from the surrounding
289 vasculature, while the vasculature of the underlying eighth cusp opens into a
290 large, central hollow. The lateral tooth row comprises around twelve cusps,
291 and its teeth are laterally unornamented and continuous with the lateral
292 surface of the dermal bone, connected to one another via antero-posterior
293 lateral ridges (figure 2b). The lingual side of each cusp is rounded, and
294 ornamented with a number of ridges, which become longer and progressively
295 more tuberculated on more anterior cusps. The lingual tooth row comprises
296 ten cusps, which curve away from the occlusal surface anteriorly.

297 Only the posteriormost portion of the Meckel's cartilage, the articular
298 ossification, is preserved (figure 2). It is formed from a sheath of perichondral
299 bone and would have been filled with cartilage in life. Some spongy texture is
300 apparent on the interior surface of the perichondral bone. A shallow groove on
301 the posterior surface does not appear to continue ventrally, making it unlikely
302 to have accommodated a mandibular splint as previously suggested [45].

303 Articulation with the palatoquadrate appear to be via an open, oval, fossa [45]
304 (figure 2d). The tissue forming this is notably ill-formed, and appears to lack a
305 solid perichondral covering; as Burrow [22] suggests it seems likely to be a
306 articular process like that in other ischnacanthids [22,25] which is broken.

307 **3.2 *Atopacanthus***

308 The dentigerous jaw bone is robust, trapezoid in cross-section, but flattened
309 laterally and taller proportionate to its length compared to *Taemasacanthus*
310 (figure 3). It is slightly medially convex. The anterior fifth of the preserved
311 bone (it is broken both anteriorly and posteriorly) is toothless and tapers
312 slightly. A narrow, shallow groove to accommodate the mandibular cartilage
313 runs along its ventral surface (figure 3c). The histology is similar to
314 *Taemasacanthus*, with heavily vascularised dermal bone surrounded by a
315 less vascular layer, but the vascular tubules are even more strongly polarised
316 in an antero-dorsal direction (figure 3e; figure S1e-g). Again, the vasculature
317 principally opens into the ventral groove. Towards the surface, bone
318 vascularisation is less dense, and not polarised. The lingual face of the
319 dentigerous jaw bone supports a distinct thin, lingual, tooth-bearing plate
320 (figure 3a,d,e), which is comparable in position and vascularisation to the
321 plate-like region in *Taemasacanthus* (figure S1d). This plate is still heavily
322 vascularised, but tubes are polarised dorso-lingually. On the outer perimeter
323 of the lateral face of the main bone, the vasculature is oriented obliquely.

324 As in *Taemasacanthus*, lateral, mesial and lingual tooth rows are borne on the
325 dorsal surface of the underlying dermal plate (figure 3a,b,d). The medial ridge
326 bears two disorganised rows of cusps along its anterior half, with the posterior
327 half being smooth. All cusps are vascular, and are histologically continuous
328 with the medial ridge. The lateral tooth row comprises eight cusps, which
329 become progressively larger anteriorly, and their lateral surfaces are
330 continuous with the outside of the dermal plate (figure 3b). Their lingual
331 surfaces are rounded and ornamented with untuberculated ridges. The lingual

332 tooth row comprises ten main cusps, which curve medially across the
333 dentigerous jaw bone. Two additional small cusps are present near the
334 posterior margin of the dermal plate, ventral to the main lingual tooth row,
335 which are closest in appearance to the teeth of the medial ridge (figure 3a,d).
336 The lingual tooth row lies on top of a lingual plate, which is apposed onto the
337 lingual surface of the main dermal plate (figure 3a,d,e) . As in the lateral row
338 and in *Taemasacanthus*, cusps become larger anteriorly, and are ornamented
339 with ridges. The histology of the teeth of the lateral and lingual rows
340 comprises a vascular base topped with an avascular cap lacking enameloid,
341 with the vascular canals oriented distinctly from the underlying dermal and
342 lingual plates (figure 3e). As in *Taemasacanthus*, younger teeth are more
343 heavily vascularised with an extensively vascularised crown, and the
344 anteriormost tooth still possesses a clear pulp cavity (figure S1e-g), suggesting
345 that teeth vasculature became infilled with age. Teeth in both the lateral and
346 lingual rows were added anteriorly, with anterior cusps partly overlying their
347 posterior fellows.

348

349 **3.3 *Ischnacanthus***

350 Only the anterior part of the dentigerous jaw bone is preserved in the part
351 (figure 4), although the mould of the posterior region is visible in outline. The
352 underlying dermal plate is much shallower than in *Taemasacanthus* and
353 *Atopacanthus*. A lateral tooth row and a medial ridge are present. The lateral
354 tooth row preserves four cusps, the third of which is exposed on the surface
355 and therefore incomplete dorsally. The cusps are linked by a cuspidate ridge
356 along their lateral faces. Relative size and age are difficult to determine due to

357 the mode of preservation, but the anteriormost cusp is the largest, and cusp
358 overlap indicates that teeth were added anteriorly. Although the ventralmost
359 parts of the dermal plate are missing, the ventral margin of the teeth is
360 marked by a noticeable shift in density and orientation of the vascular canals
361 (figure 4d). The tissue forming the teeth is similar to *Taemasacanthus* and
362 *Atopacanthus*, with a vascularised base and an avascular crown apparently
363 lacking enameloid [22]. The internal vasculature of the bone in *Ischnacanthus*
364 is also longitudinally polarised and connected, although less well-visualised in
365 our scan data (figure S1h,i).

366 The large Meckel's cartilage is near-complete and preserved as a single
367 ossification (figure 4). It is curved posteriorly and tapers anteriorly. The
368 dentigerous jaw bone is borne on its dorso-lingual surface. A laterally-directed
369 articular condyle is present at the posterior extent, and a shallow groove
370 extends ventral to the condyle. The majority of the Meckel's cartilage is
371 formed of globular calcified cartilage. Parts of its lateral surface, as well as its
372 ventral, anterior, and posterior extents, are covered by a thin, densely
373 mineralised tissue that appears to be perichondral bone [22]. This tissue
374 thickens ventrally and posteriorly and is fractured. The perichondral sheath is
375 avascular, but has fractured in such a way that cracks and voids artificially
376 resemble the vasculature of the dentigerous jaw bone. A thickened ridge
377 along the posteroventral and posterior margin is continuous with the
378 perichondral rind that extends onto the lateral surface, but externally gives the
379 appearance of a separate ossification (figure 4bc,). In section this is closely
380 comparable to the so called "mandibular bone" that Ørvig [39] described in

381 *Xylacanthus and* is probably responsible for accounts of mandibular splints in
382 ischnacanthids.

383 **3.4 *Acanthodopsis***

384 The lower jaw in *Acanthodopsis* comprises a tooth-bearing Meckel's cartilage
385 and a mandibular splint (figure 5). The Meckel's cartilage is long and thin and
386 similar in form to that of *Acanthodes* (figure 5; 23,54], with an identical
387 articular cotylus and marked preglenoid process. It tapers anteriorly,
388 terminating in a small, cup-shaped anterior symphyseal fossa (figure 5c,e).
389 The Meckel's cartilage is formed from a shell of what we infer to be
390 perichondral bone [23], which has collapsed and cracked under compression
391 and appears to be unmineralized internally (figure 5g,h), although some
392 mineralisation appears to be present in the jaw articulation. Unlike
393 *Acanthodes confusus*, it is perichondrally mineralised along its entire length
394 (figure 5), rather than in separate articular and mentomandibular sections.

395 Ten monocuspid, triangular teeth form a row along the dorsal surface of the
396 Meckel's cartilage (figure 5). The largest tooth is in the middle of the jaw, with
397 teeth becoming smaller and more closely set anteriorly and posteriorly; they
398 are slightly lingually convex, each with a smooth (but possibly weathered)
399 lateral face and a longitudinally striated lingual face. Previous descriptions of
400 the teeth [23] were undecided as to their tissue makeup. The tissue
401 comprising them comprises distinct inner and outer layers. The outer layer is
402 thick and covers the outside surface of each tooth but does not close
403 ventrally: unlike the perichondral surface of the cartilage it is not crushed and
404 the surface appears intact. The inner layer has a spongy texture, which may
405 reflect internal vasculature: no obvious pulp canals are present. Although the

406 contrast between the teeth and jaw bone is subtle, they can be differentiated
407 in that the internal tissues of the teeth have a spongy texture, whereas the
408 perichondral bone is solid. We infer the teeth to be dermal due to this
409 histological distinction from the Meckel's cartilage as well as their gross
410 structure, which shows a separation from the Meckel's cartilage, and their
411 ornamentation. We consider it likely that these tissues are dentinous but more
412 detailed study is needed to establish their identity. The direction of growth is
413 difficult to infer. In successive tomograms viewed in sequence, the largest
414 tooth appears to be overlapped by the anterior and posterior teeth, possibly
415 making it the oldest. This contrasts to the order of growth in *Taemasacanthus*,
416 *Atopacanthus* and *Ischnacanthus*, where teeth are added anteriorly. However,
417 as with the identity of the tissue, we express caution at this interpretation.

418 The mandibular splint in *Acanthodopsis* is an unornamented, slightly
419 sinusoidal bone that fits into a groove on the ventro-lateral part of Meckel's
420 cartilage, extending almost its entire length (figure 5a,b). This groove was
421 likely originally much shallower, and its depth has been exaggerated by lateral
422 flattening of the specimen. The tissue forming the splint is solid, and is
423 organised into multiple concentric lamellae likely representing lines of arrested
424 growth. It is pierced by a series of thin, longitudinally oriented canals (figure
425 5g,h). This tissue is distinct from that forming Meckel's cartilage, in particular
426 being denser and better organised, and can be interpreted as dermal bone,
427 especially given the ornamentation of the mandibular splints of some
428 acanthodids [57]. Burrow [23] reported that the mandibular splint in
429 *Acanthodopsis* was formed from cartilage and bone based on thin sections,

430 but the cartilage identified in these reports may have been the Meckel's
431 cartilage above the bone instead (CJB pers. comm. July 2020).

432

433 **3.2 *Acanthodes***

434 The left lower jaw comprises ossified articular and mentomandibular parts of
435 Meckel's cartilage, as well as a mandibular splint (figure 6). Mineralised parts
436 of the Meckel's cartilage are formed from thick perichondral bone, and are
437 slightly laterally crushed (figure. 6a-d). The articular is as previously described
438 [54]. The mentomandibular has a distinct cup-like symphyseal fossa at its
439 anterior tip, forming part of the mandibular symphysis (figure 6c). The
440 mandibular splint is unornamented, slightly sinusoidal in shape, and ellipsoid
441 in cross-section. It sits in a groove in the lateral faces of the mentomandibular
442 and articular. Internally it is solid and vascularised by sparse long, thin canals
443 running its length (figure 6e,f), as in *Acanthodopsis*. A single tooth-like cusp
444 sitting in (although separate from) a cushion-shaped base is probably a
445 branchial or hyoid raker (figure 6b,e).

446

447 **3.6 *Phylogenetic results***

448 Our parsimony analysis recovered 26101 most parsimonious trees with a
449 length of 704 steps. The strict consensus of these results (figures 7a, S2) is
450 consistent with other recent analyses in finding all 'acanthodians' to be stem-
451 group chondrichthyans. We recover "Acanthodii" *sensu* Coates *et al.* [24] as a
452 clade subtending the remainder of the chondrichthyan total group, with
453 *Euthacanthus* as the sister group to the "Acanthodii". However,

454 acanthodiforms (i.e. cheiracanthids, mesacanthids, and acanthodids) are
455 paraphyletic. Ischnacanthids plus diplacanthids form a clade, but
456 ischnacanthids themselves are paraphyletic, and diplacanthids are a clade to
457 the exclusion of *Tetanopsyrus*. Remaining stem chondrichthyan taxa,
458 including climatiids, *Gladbachus* and *Doliodus*, are recovered in a polytomy
459 along with a monophyletic chondrichthyan crown group. Support values aside
460 from the chondrichthyan total group and crown group nodes are typically low.
461 The Bayesian majority rule consensus tree (figure 7b, S3) is broadly
462 consistent with the parsimony strict consensus tree, although “Acanthodii” is
463 instead recovered as a polytomy subtending all more crownwards
464 chondrichthyans. *Acanthodopsis* is recovered as the sister-taxon to
465 *Acanthodes* in both analyses.

466

467

468 **4. Discussion**

469 **4.1 Stem-chondrichthyan oral structures**

470 Our new data show that the dentigerous jaw bones of all ischnacanthids,
471 including articulated taxa such as *Ischnacanthus* and those only known from
472 isolated jaws (e.g. atopacanthids and taemasacanthids), were united by a
473 common construction. These follow the model of tooth growth hypothesized
474 by Ørvig [26] and demonstrated by Rucklin *et al.* [7] on the basis of directional
475 wear and overlapping cusps. These teeth were fused to, but distinct from, the
476 underlying bone, which grew with the endoskeletal component of the jaw.
477 Based on the vasculature of *Taemasacanthus* the dermal bone grew radially

478 from a point posterior to the tooth row. This condition and the positions of
479 tooth rows relative to the underlying dermal plate is common to the three
480 different morphologies of dentigerous jaw bone that we describe and we infer
481 it to have been a common feature of ischnacanthid dentigerous jaw bones
482 The presence of an out of sequence tooth in *Taemasacanthus*, where the
483 youngest tooth has partially overgrown a cusp anteriorly (figure 2), suggests
484 that non-sequential growth was possible in the otherwise ordered tooth rows,
485 likely in response to a pathology. Dentigerous jaw bones are broadly
486 comparable with the condition in stem-gnathostomes in the sense that non-
487 shedding teeth are ankylosed to and growing on a basal bone. However,
488 phylogenetic topologies supporting homology between these conditions are in
489 limited supply (figures 7,8), and is not upheld in our topology or by more
490 detailed analysis [7].

491 Although dentigerous jaw bones are typically contrasted with tooth whorls [7],
492 we suggest that dentigerous jaw bones can be usefully interpreted by
493 comparison to antero-posteriorly “stretched out” tooth whorls. Teeth and
494 tooth-like structures are added directionally across the gnathostome total-
495 group and this may be a plesiomorphic feature of gnathostome dentitions [6].
496 However, tooth rows on dentigerous jaw bones are more comparable to
497 whorls than to these other structures in that tooth files are located in a specific
498 position on an underlying dermal plate, growing in a single direction. This
499 stands in contrast to single-directional, but haphazardly arranged, tooth files
500 reported in stem-gnathostomes and early osteichthyan marginal jaw bones
501 [6,9]. Notably, symphyseal tooth whorls and whorl-like cheek scales in some
502 ischnacanthids could suggest common patterning mechanisms affecting

503 dermal structures in and around the mouth of early chondrichthyans [58]. This
504 organisation tooth files could be apomorphic for chondrichthyans if
505 osteichthyan tooth whorls are optimised as homoplasious [7], and could
506 potentially be a character uniting chondrichthyan dentitions more inclusively
507 than the presence of tooth whorls.

508 The row of monocuspid ‘teeth’ borne directly on the Meckelian element of
509 *Acanthodopsis* is unlike that of any other known chondrichthyan or
510 gnathostome. Furthermore, the presence of teeth in a Carboniferous taxon
511 deeply nested within an edentulous radiation (figure 7), the oldest of which are
512 Early Devonian in age, strongly suggests that this represents an independent
513 acquisition of dentition. Previous studies of the jaw of *Acanthodopsis* have
514 interpreted it either as a dentigerous jaw bone [26] or as a perichondrally
515 ossified Meckelian bone with ‘teeth’ [23]. Our data confirm the latter view and
516 show that the teeth in *Acanthodopsis* are histologically distinct from the
517 underlying perichondral bone and so are presumably dermal ossifications
518 attached to its surface. Our phylogenetic analysis supports the view of Long
519 [45] and Burrow [23] that *Acanthodopsis* is closely related to *Acanthodes*, with
520 the presence of teeth representing the only difference between the genera. A
521 possible morphological comparison to these teeth lies in the branchial and
522 hyoid rakers found in acanthodiform fishes like *Acanthodes*, *Cheiracanthus*,
523 and *Homalacanthus* [31,59]. As with the teeth of *Acanthodopsis*, these rakers
524 are conical, sometimes striated ([61] fig. 3), and decrease in size from the
525 centre outwards (Dearden *pers obs*). An alternative to homology between
526 the mandibular dentition in *Acanthodopsis* and other gnathostomes, which is
527 difficult to reconcile with their phylogenetic relationships, may be the co-option

528 of hyoid and branchial rakers to form a novel “dentition” on the mandibular
529 arch.

530 **4.2 Distribution of oral structures in the chondrichthyan stem-group**

531 Teeth and other oral structures in stem-chondrichthyans take on a broad
532 variety of forms, raising questions about their homology and the primitive or
533 derived condition for different features. Here we briefly review this diversity
534 and map key characters onto our phylogeny.

535 A diverse array of **teeth** (light blue icons, figures 7 and 8) are present in the
536 majority of Palaeozoic chondrichthyans, including as tooth whorls, but are
537 also remarkable for the breadth of taxa in which they are absent. Acanthodids
538 (e.g. *Acanthodes*: figure 6, ref. [54]) are completely toothless, except for
539 *Acanthodopsis*, as are the likely related mesacanthids (e.g. *Promesacanthus*
540 [37]) and cheiracanthids (e.g. *Cheiracanthus* [59]). In this latter group, tooth-
541 like hyoid rakers have sometimes been mistaken for teeth [61]. Teeth are also
542 absent in diplacanthids [28], with the possible exception of *Tetanopsyrus* (see
543 “Occlusal plates” section below) [29]. A number of toothless taxa with
544 otherwise diverse anatomies, including *Obtusacanthus*, *Lupopsyrus*,
545 *Euthacanthus*, *Brachyacanthus*, and *Kathemacanthus* [62-65], are often
546 resolved as more closely related to the crown-group (figures 7,8). Given the
547 small size and two-dimensional preservation of some of these taxa, it is
548 possible that teeth are present but reduced and so far undetected, as in
549 *Gladbachus adentatus* [24]. Teeth are inferred to be homologous across
550 gnathostomes [7], demanding numerous independent losses of teeth in stem
551 chondrichthyans (figures 7 and 8).

552 **Tooth whorls** (dark green icons, figures 7 and 8) are tooth files with a fused
553 bony base, which grow by the lingual addition of new cusps along a single
554 axis [20]. Tooth whorls are understood to be the evolutionary precursor to
555 modern chondrichthyan tooth families, which have a similar morphology but
556 lack a common bony base [66]. Tooth whorls are present in a range of stem-
557 group chondrichthyans with otherwise dissimilar anatomies, including those
558 with dentigerous jaw bones (e.g. *Ischnacanthus* [22]), densely tessellate head
559 skeletons (e.g. *Climatius* [67]), and more conventionally shark-like taxa (e.g.
560 *Doliodus* [17]). They have also been described in the acanthodiform-like
561 *Latviacanthus* [68], although as this is based on x-ray plates these may be
562 mischaracterised hyoid rakers as in *Homalacanthus* [59]. Tooth whorls are
563 also present in some stem-group holocephalans such as iniopterygians [69],
564 although these are likely to be secondarily derived given their phylogenetic
565 remoteness from the chondrichthyan stem-group. Some osteichthyan taxa
566 also possess tooth whorls, but here the tooth crowns are shed via resorption
567 of the tooth base, a mechanism not present in statodont chondrichthyan tooth
568 whorls [14]. There is variation in their distribution on the jaw: in ischnacanthids
569 and osteichthyans, tooth whorls are few in number and limited to the
570 symphysis [22], whereas in more crownward chondrichthyans they are
571 arrayed along the length of the jaw and comprise the entire dentition (gold and
572 yellow-green icons, figures 7 and 8). The distribution of tooth whorls across
573 osteichthyans and within chondrichthyans is complex, with whorl-bearing taxa
574 often nested within whorl-less radiations. Probabilistic ancestral state
575 reconstruction indicates that tooth whorls evolved independently multiple
576 times both within chondrichthyans and across gnathostomes [7]. Within

577 chondrichthyans, different phylogenetic topologies have quite different
578 implications for the gain and loss of tooth whorls and their distribution across
579 the group (figure 8).

580 Some chondrichthyans have **teeth that are not organised into files** but
581 which lie directly on the jaw cartilage (coral icons [in part; this icon also
582 captures teeth arranged in files that are borne on the jaw cartilages], figures 7
583 and 8). This condition is present in *Acanthodopsis* (figure 5), *Pucapampella*,
584 and *Gladbachus* [18,24], although expressed in different ways. In
585 *Acanthodopsis*, teeth are triangular in profile and diminish in size anteriorly
586 and posteriorly (figure 5). In *Pucapampella*, teeth form a single row along the
587 jaw but show a variety of sizes, shapes, and spacings [18]. In *Gladbachus*,
588 teeth are much reduced and individually separate, although possibly aligned
589 linguo-labially [24]. However, these taxa are scattered across the tree, and
590 their tooth morphologies can be radically different, suggesting that teeth that
591 lie directly on the jaw cartilage and are not organised into files evolved
592 multiple times independently. Although *Gladbachus* and *Pucapampella* are
593 recovered as a clade in our analyses, this is contrary to most other recent
594 findings (figure 8c,d) and we view this result with extreme caution.

595 **Dentition cones** are tooth-like cones with smaller denticles attached. They
596 are only known in three partially-articulated ischnacanthids (*Zemylacanthus*
597 (*Poracanthodes*), *Acritolepis*, and *Serradentus* [52,70,71]), and are absent in
598 the better characterised *Ischnacanthus* and relatives [22,58]. The lack of fully
599 articulated fossils bearing dentition cones leaves open the possibility that they
600 represent a displaced part of the branchial apparatus rather than oral
601 structures [50], and are perhaps comparable to gill and hyoid rakers in

602 cheiracanthids and acanthodids [31,59]. Whether oral or branchial in origin,
603 their presence may unite the subset of ischnacanthids that possess them,
604 although this has not been tested in a phylogenetic context.

605 **Tooth-like scales** are present along the oral margin of some stem-group
606 chondrichthyans, and include part of the cheek squamation, the 'lip' and the
607 ventral rostral area. They are best characterised in *Ischnacanthus*-like
608 'acanthodians' [32] in which they show a variety of morphologies, and in life
609 may have helped with grasping prey. Some of these scales are strikingly
610 similar in organisation to tooth whorls (which are also present within the gape
611 of the same animals), comprising a file of denticles oriented towards the
612 mouth [22,32]. Specialised tooth-like scales have also been identified along
613 the margin of the mouth in *Obtusacanthus* [63]. More generally, tooth-like
614 denticles are common along the oral margin of the tooth row in early
615 osteichthyans [14,72]. Although potentially interesting from a developmental
616 perspective, they seem unlikely to carry any phylogenetic signal.

617 **Dentigerous jaw bones** are tooth-bearing dermal jaw bones present in the
618 upper and lower jaws of a number of stem-chondrichthyan taxa [23].
619 Articulated fossils bearing dentigerous jaw bones include *Zemlyacanthus*,
620 *Nerepisacanthus*, and *Serradentus* [44,52,73]. By far the best anatomically
621 characterised taxa with dentigerous jaw bones are *Ischnacanthus* and similar
622 taxa [22,25]. There are few anatomical characters to group taxa possessing
623 dentigerous jaw bones, but all have a complement of oral structures including
624 some combination of symphyseal tooth whorls, dentition cones, and tooth-like
625 cheek scales. Dentigerous jaw bones themselves display anatomical diversity,
626 for example relating to the structure of the bone, the number and morphology

627 of tooth rows [23], and variance in dentition shapes likely linked to diet [25]. In
628 our phylogeny, taxa with dentigerous jaw bones (i.e. ischnacanthids) are
629 recovered in a polytomy, in a broader grouping of ‘acanthodians’ with dermal
630 mouth plates (dark purple icons, figures 7 and 8). Dermal jaw bones, both
631 edentulous and tooth-bearing, are also present in ‘placoderms’ and
632 osteichthyans, but few phylogenetic results support their homology with those
633 of ischnacanthids (Fig. 7,8).

634 **Occlusal plates** are a pair of smooth dermal plates in the gapes of some
635 stem-chondrichthyans (light purple icons, figures 7 and 8). Their detailed
636 anatomy is poorly characterised and in the past they have become
637 terminologically and anatomically confused with the mandibular splint [30].
638 Occlusal plates are present in *Diplacanthus*, *Rhadinacanthus*, *Milesacanthus*,
639 *Uraniacanthus*, *Culmacanthus*, and *Tetanopsyrus* [28-30,74–76]. At least
640 some of these taxa have other common morphologies (i.e. similar body
641 shapes, scapular processes with posterior lamina, large postorbital scales,
642 deep, striated dorsal fin spine insertions), and on this basis they are grouped
643 into the diplacanthids [28]. There is some variation in the morphology of
644 occlusal plates. In all taxa but *Tetanopsyrus* [29,77], they are only present in
645 the lower jaws. *Tetanopsyrus* may also have tooth-like denticles along the
646 inner surface of the plates, although this is only known from an isolated
647 Meckel’s cartilage associated with a complete *Tetanopsyrus* specimen [29]
648 and its attribution is therefore uncertain. In *Uraniacanthus* and *Culmacanthus*,
649 a dorsal process is present [74,78]. We recover diplacanthids as monophyletic
650 in our Bayesian analysis (figure 7, S3), but paraphyletic with respect to
651 *Tetanopsyrus* in our parsimony analysis, and occlusal plates appear to be a

652 character uniting diplacanthids (figures 7, 8). *Tetanopsyrus*, with its upper and
653 lower plates, may represent a link between the occlusal plates of
654 diplacanthids and dermal jaw bones of ischnacanthids.

655 A **mandibular splint** (variously termed dentohyoid, extramandibular spine,
656 splenial, or mandibular bone) is a slightly sinusoidal dermal bone that
657 underlies the Meckel's cartilage ventrolaterally (grey icons, figures 7 and 8).
658 Unlike the other structures discussed here, it did not lie within the gape, and
659 likely reinforced the lower jaw. Mandibular splints are present in *Acanthodes*,
660 *Acanthodopsis*, *Halimacanthodes*, *Howittacanthus*, and *Protogonacanthus*
661 [55,57,79,80]. They have also been incorrectly identified in a variety of other
662 taxa. Mandibular splints in mesacanthids [35,62] are more similar in size to
663 gular plates, and may represent displaced elements of this series. Reports in
664 diplacanthids [74,76] are better interpreted as occlusal plates [30]. Although a
665 mandibular splint has been identified in the putative cheiracanthid
666 *Protogonacanthus* [57], the taxon in question is likely not a cheiracanthid but
667 an acanthodid [59]. Finally, as we show, descriptions of mandibular splints in
668 ischnacanthids [39,50] instead represent a reinforced ventral margin of the
669 endoskeletal mandible. Mandibular splints in acanthodids are very
670 conservative in form, although may be ornamented as in *Acanthodes sulcatus*
671 [57]. Its similarity to the ventral branchiostegal rays in *Acanthodes* (figure
672 6a,b), which are also dermal, tubular, and slightly sinusoidal, suggests that it
673 may be part of this series that has been co-opted to support the jaw. Our
674 phylogeny suggests that a mandibular splint unites *Acanthodes* and
675 *Acanthodopsis* but either evolved convergently in *Halimacanthodes* (figure. 7)
676 or was lost in *Homalacanthus*; we consider it most likely that it unites

677 acanthodids to the exclusion of other stem-chondrichthyans, and that this
678 distribution is a result of undersampling acanthodids and their characters in
679 our phylogeny.

680 **4.3 The evolution of chondrichthyan teeth**

681 Although phylogenetic topologies for early chondrichthyans are poorly
682 resolved and often suggest conflicting hypotheses, there are some signals
683 that may provide insight into the evolution of a modern shark-like dentition.
684 The placement of 'climatiid' acanthodians in a relatively crownward position
685 on the chondrichthyan stem [24,42-44] (Fig. 7,8a-c) suggests that taxa with a
686 dentition entirely formed from tooth whorls share a last common ancestor to
687 the exclusion of other stem-group chondrichthyan taxa. Not all topologies
688 support this hypothesis, however: Frey *et al.* [35] recover climatiids as remote
689 from the chondrichthyan crown node, implying that an extensively whorl-
690 based dentition borne on the jaw cartilages either developed independently in
691 the crownward lineage or was lost in the *Acanthodii sensu* Coates *et al.* This
692 phylogeny is based on a more limited selection of stem-group chondrichthyan
693 taxa, which may have had an influence on reconstructed patterns of character
694 evolution. Either scenario still invokes multiple episodes of secondary tooth
695 loss (e.g. *Lupoposyrus*) and divergences from a whorl-like tooth anatomy
696 (*Gladbachus*, *Pucapampella*). In our phylogeny, tooth-shedding is restricted to
697 the crown-node. Generative tooth series are present in stem-group
698 elasmobranchs (e.g. *Phoebodus* [34]) and stem-group holocephalans with
699 both shark-like (e.g. *Ferromirum* [35]) and more chimaeroid-like (e.g.
700 *Debeerius* [81]) forms. However, it is unclear how widespread the non-
701 shedding condition described in some sharks with cladodont teeth [36] is.

702 Either way, this suggests a ‘two-step’ development of the stereotypical
703 chondrichthyan dentition, with an initial shift towards tooth whorls borne
704 exclusively on the jaw cartilages, followed by the eventual loss of fused bases
705 and concomitant development of tooth shedding in crown-group
706 chondrichthyans. However, significant phylogenetic uncertainty persists, and
707 this scenario warrants further testing as hypotheses of relationship stabilise.
708 Despite this, the interposition of multiple lineages of non-shedding stem-
709 chondrichthyan taxa between shedding chondrichthyans and shedding
710 osteichthyans confirms that a shedding dentition evolved twice, in two
711 different ways, in crown-gnathostomes [6,7,11,14].

712 In stark contrast to the clade comprising chondrichthyans with tooth whorls,
713 the clade or grade including diplacanthids, acanthodids, and
714 ischnacanthiforms exhibits a diverse array of oral structures, none of which
715 seem to persist beyond the end of the Palaeozoic [24]. In phylogenetic
716 analyses, this grade is consistently recovered at the base of the
717 chondrichthyan total-group, with the exception of Frey *et al.* [35], who recover
718 it in a more crownward position. A number of likely apomorphic oral
719 morphologies are present within this clade, including diplacanthid occlusal
720 plates, ischnacanthid dentigerous jaw bones and toothless acanthodids with
721 mandibular splints. Many of these morphologies are known from the Late
722 Silurian and Devonian, approximately contemporaneously to ‘acanthodians’
723 with tooth whorls and the unusual dentitions in more shark-like taxa (e.g.
724 *Pucapampella*, *Gladbachus*). Novel oral morphologies have been linked to a
725 period of inferred rapid gnathostome evolution [7,43]. Furthermore, in the
726 Devonian small-bodied chondrichthyans were significant in freshwater

727 nektonic faunas [24]: diverse oral structures seem likely to have accompanied
728 their radiation into these niches. While the latest surviving lineage of the
729 ‘acanthodian’ grade was the remarkably morphologically conservative
730 acanthodids [79], *Acanthodopsis* shows that experimentation with novel oral
731 apparatus in stem-group chondrichthyans continued well into the Late
732 Carboniferous.

733 **4. Summary**

734 ‘Acanthodian’ stem-group chondrichthyans display a diverse array of oral and
735 dental morphologies, including an apparently independent origin of teeth deep
736 within an edentulous clade. However, interpreting patterns of tooth evolution
737 is complicated by conflicting and unresolved phylogenetic hypotheses, both
738 for the chondrichthyan (figure 7; figures S1,2) and gnathostome stem-group
739 (e.g. [6,43]). CT- and synchrotron-based investigations seem likely to provide
740 the anatomical information necessary to resolve these instabilities, and
741 likelihood-based methods provide another potential way of overcoming
742 uncertainties [7]. In the meantime, the proliferation of different tree shapes in
743 conjunction with generally low support values means that morphologies
744 should be considered across multiple potential topologies. This illustrates the
745 challenges of drawing broad scale conclusions for gnathostome tooth
746 evolution on the basis of unstable relationships or tentatively placed taxa.

747

748 **Acknowledgements**

749 We thank E. Bernard and Z. Johanson (NHMUK) for assistance with
750 specimen access, V. Fernandez and B. Clark (both NHMUK) and T. Davies
751 (University of Bristol) for assistance with CT scanning. M. Brazeau (Imperial
752 College London), B. Davidson, and C. Burrow (Queensland Museum) and P.
753 Ahlberg (Uppsala University) contributed to helpful discussion. M. Colfer
754 (University of Oxford) carried out preliminary segmentation and interpretation
755 of the Mimics files. Four anonymous reviewers provided helpful comments,
756 and we also thank two anonymous reviewers for their comments on an earlier
757 version of this manuscript.

758 **Funding**

759 This work was supported by a Junior Research Fellowship, Christ Church,
760 Oxford, and a Royal Society Dorothy Hodgkin Research Fellowship, both to
761 S.G.. R.P.D. was supported by a Paris Île-de-France Région – DIM
762 “Matériaux anciens et patrimoniaux” grant (PHARE project).

763

764 **Ethics.** This research is based exclusively on specimens from natural history
765 collections.

766 **Data accessibility.** Raw data (.vol or .tiff stacks), Mimics files, and 3D PLY
767 files for each specimen are deposited in Zenodo (10.5281/zenodo.5238205).

768 **Authors' contributions.** S.G. conceived the project and selected specimens.
769 S.G. and R.P.D. carried out CT scanning. R.P.D. segmented the specimens,
770 made Blender renders and constructed figures with input from S.G. S.G. and
771 R.P.D. drafted the manuscript. Both authors revised and edited the

772 manuscript, approved the final version and agree to be accountable for all

773 aspects of the work.

774 **Competing interests.** We have no competing interests.

775

776

777

778 **5. References**

- 779 1. Tucker AS, Fraser GJ. 2014 Evolution and developmental diversity of
780 tooth regeneration. *Semin. Cell Dev. Biol.* **25–26**, 71–80.
781 (doi:10.1016/j.semcdb.2013.12.013)
- 782 2. Jobbins M, Rücklin M, Argyriou T, Klug C. 2021 A large Middle Devonian
783 eubranchyothoracid ‘placoderm’ (Arthrodira) jaw from northern Gondwana.
784 *Swiss J. Palaeontol.* **140**, 2. (doi:10.1186/s13358-020-00212-w)
- 785 3. Ørvig T. 1980 Histologic Studies of Ostracoderms, Placoderms and Fossil
786 Elasmobranchs: 3. Structure and growth of the gnathalia of certain
787 arthrodiras. *Zool. Scr.* **9**, 141–159. (doi:10.1111/j.1463-
788 6409.1980.tb00660.x)
- 789 4. Rücklin M, Donoghue PCJ. 2015 *Romundina* and the evolutionary origin of
790 teeth. *Biol. Lett.* **11**, 0–4.
- 791 5. Rücklin M, Donoghue PCJ, Johanson Z, Trinajstić K, Marone F,
792 Stampanoni M. 2012 Development of teeth and jaws in the earliest jawed
793 vertebrates. *Nature* (doi:10.1038/nature11555)
- 794 6. Vaškaninová V, Chen D, Tafforeau P, Johanson Z, Ekrt B, Blom H,
795 Ahlberg PE. 2020 Marginal dentition and multiple dermal jawbones as the
796 ancestral condition of jawed vertebrates. *Science* **369**, 211–216.
797 (doi:10.1126/science.aaz9431)
- 798 7. Rücklin M, King B, Cunningham JA, Johanson Z, Marone F, Donoghue
799 PCJ. 2021 Acanthodian dental development and the origin of
800 gnathostome dentitions. *Nat. Ecol. Evol.*, **14**. (doi: 10.1038/s41559-021-
801 01458-4)
- 802 8. Hu YZ, Young GC, Burrow CJ, an Zhu Y, Lu J. 2018 High resolution XCT
803 scanning reveals complex morphology of gnathal elements in an Early
804 Devonian arthrodira. *Palaeoworld* (doi:10.1016/j.palwor.2018.12.003)
- 805 9. Botella H, Blom H, Dorka M, Ahlberg PE, Janvier P. 2007 Jaws and teeth
806 of the earliest bony fishes. *Nature* **448**, 583–586.
807 (doi:10.1038/nature05989)
- 808 10. Chen D, Blom H, Sanchez S, Tafforeau P, Ahlberg PE. 2016 The stem
809 osteichthyan *Andreolepis* and the origin of tooth replacement. *Nature*
810 (doi:10.1038/nature19812)
- 811 11. Chen D, Blom H, Sanchez S, Tafforeau P, Märss T, Ahlberg PE. 2017
812 Development of cyclic shedding teeth from semi-shedding teeth : the inner
813 dental arcade of the stem osteichthyan *Lophosteus* R. *Soc.*
814 *open sci.* **4**: 161084.
- 815 12. Chen D, Blom H, Sanchez S, Tafforeau P, Märss T, Ahlberg PE. 2020 The
816 developmental relationship between teeth and dermal odontodes in the

- 817 most primitive bony fish *Lophosteus*. *eLife* **9**, e60985.
818 (doi:10.7554/eLife.60985)
- 819 13. Cunningham JA, Rücklin M, Blom H, Botella H, Donoghue PCJ. 2012
820 Testing models of dental development in the earliest bony vertebrates,
821 *Andreolepis* and *Lophosteus*. *Biol. Lett.* **8**, 833–837.
822 (doi:10.1098/rsbl.2012.0357)
- 823 14. Doeland M, Couzens AMC, Donoghue PCJ, Rücklin M. 2019 Tooth
824 replacement in early sarcopterygians. *R. Soc. Open Sci.* **6**.
- 825 15. Zhu M, Ahlberg P E, Pan, Z, Zhu Y, Qiao T, Zhao W, Jia L, Lu J. 2016 A
826 Silurian maxillate placoderm illuminates jaw evolution. *Science* **354** 6310
827 334–336.
- 828 16 Zhu Y, Ahlberg, P A, Zhu M. 2018 The evolution of vertebrate dermal jaw
829 bones in the light of maxillate placoderms. In *Evolution and Development*
830 *of Fishes* (Ed. Zerina Johanson) 71–86.
- 831 17. Maisey JG, Turner S, Naylor GJP, Miller RF. 2014 Dental patterning in the
832 earliest sharks: Implications for tooth evolution. *J. Morphol.* **275**, 586–96.
833 (doi:10.1002/jmor.20242)
- 834 18. Maisey JG, Janvier P, Pradel A, Denton JSS, Bronson A, Miller RF,
835 Burrow CJ. 2019 *Doliodus* and pucapampellids: contrasting perspectives
836 on stem chondrichthyan morphology. In *Evolution and Development of*
837 *Fishes* (eds Z Johanson, C Underwood, M Richter), pp. 87–109.
838 Cambridge: Cambridge University Press.
- 839 19. Qu Q, Sanchez S, Blom H, Tafforeau P, Ahlberg PE. 2013 Scales and
840 Tooth Whorls of Ancient Fishes Challenge Distinction between External
841 and Oral ‘Teeth’. *PLoS ONE* **8**. (doi:10.1371/journal.pone.0071890)
- 842 20. Rücklin M, Giles S, Janvier P, Donoghue PCJ. 2011 Teeth before jaws?
843 Comparative analysis of the structure and development of the external
844 and internal scales in the extinct jawless vertebrate *Loganellia scotica*.
845 *Evol. Dev.* **13**, 523–532. (doi:10.1111/j.1525-142X.2011.00508.x)
- 846 21. Miles RS. 1973 Articulated acanthodian fishes from the Old Red
847 Sandstone of England, with a review of the structure and evolution of the
848 acanthodian shoulder girdle. *Bulletin of the British Museum (Natural*
849 *History). Geology.* **24**, 111–213.
- 850 22. Burrow CJ, Newman MJ, den Blaauwen J, Jones R, Davidson RG. 2018
851 The Early Devonian ischnacanthiform acanthodian *Ischnacanthus gracilis*
852 (Egerton, 1861) from the Midland Valley of Scotland. *Acta Geol. Pol.* **68**,
853 335–362. (doi: 10.1515/agp-2018-0008)
- 854 23. Burrow CJ. 2004 Acanthodian fishes with dentigerous jaw bones : the
855 *Ischnacanthiformes* and *Acanthodopsis*. *Foss. Strata* , 8–22.
- 856

- 857
858 24. Coates MI, Finarelli JA, Sansom IJ, Andreev PS, Criswell KE, Tietjen K,
859 Rivers ML, Riviere PJJ, Coates MI. 2018 An early chondrichthyan and the
860 evolutionary assembly of a shark body plan. *Proc. R. Soc. B Biol. Sci.* **285**.
- 861 25. Blais SA, Hermus CR, Wilson MVH. 2015 Four new Early Devonian
862 ischnacanthid acanthodians from the Mackenzie Mountains, Northwest
863 Territories, Canada: an early experiment in dental diversity. *J. Vertebr.*
864 *Paleontol.* **35**, 37–41. (doi:10.1080/02724634.2014.948546)
- 865 26. Ørvig T. 1973 Acanthodian dentition and its bearing on the relationships of
866 the group. *Palaeontogr. Abt. A* **143**, 119–150.
- 867 27. Smith, MM. 2003 Vertebrate dentitions at the origin of jaws: when and how
868 pattern evolved. *Evolution & Development.* **5**(4) 394–413 (doi:
869 10.1046/j.1525-142X.2003.03047.x)
- 870 28. Burrow CJ, Blaauwen JD, Newman MJ, Davidson RG. 2016 The
871 diplacanthid fishes (Acanthodii, Diplacanthiformes, Diplacanthidae) from
872 the Middle Devonian of Scotland. *Palaeontol. Electron.* , 1–83.
- 873 29. Hanke GF, Davis SP, Wilson MVH. 2001 New species of the acanthodian
874 genus *Tetanopsyrus* from northern Canada, and comments on related
875 taxa. *J. Vertebr. Paleontol.* **21**, 740–753.
- 876 30. Newman MJ, Davidson RG, Blaauwen JLD, Burrow CJ. 2012 The Early
877 Devonian Acanthodian *Uraniacanthus curtus* (Powrie , 1870) n . comb .
878 from the Midland Valley of Scotland. *Geodiversitas* **34**, 739–759.
- 879 31. Zidek J. 1976 Kansas Hamilton Quarry (Upper Pennsylvanian)
880 *Acanthodes*, with remarks on the previously reported North American
881 occurrences of the Genus. *Univ. Kans. Palaeontol. Contrib.* , 1–41.
- 882 32. Blais SA, MacKenzie LA, Wilson MVH. 2011 Tooth-like scales in Early
883 Devonian eugnathostomes and the outside-in hypothesis for the origins of
884 teeth in vertebrates. *J. Vertebr. Paleontol.* **31**, 1189–1199.
885 (doi:10.1080/02724634.2011.607992)
- 886 33. Meredith Smith M, Underwood C, Goral T, Healy C, Johanson Z. 2019
887 Growth and mineralogy in dental plates of the holocephalan *Harriotta*
888 *raleighana* (Chondrichthyes): Novel dentine and conserved patterning
889 combine to create a unique chondrichthyan dentition. *Zoological Letters* **5**,
890 1–30. (doi:10.1186/s40851-019-0125-3)
- 891 34. Frey L, Coates MI, Ginter M, Hairapetian V, Rücklin M, Jerjen I, Klug C.
892 2019 The early elasmobranch *Phoebodus* :phylogenetic relationships,
893 ecomorphology and a new time-scale for shark evolution. *Proceedings of*
894 *the Royal Society B: Biological Sciences* **286**. (doi:
895 10.1098/rspb.2019.1336)

- 896 35. Frey L, Coates MI, Tietjen K, Rücklin M, Klug C. 2020 A symmoriiform
897 from the Late Devonian of Morocco demonstrates a derived jaw function in
898 ancient chondrichthyans. *Commun. Biol.* **3**, 681. (doi:10.1038/s42003-020-
899 01394-2)
- 900 36. Williams ME. 2001 Tooth retention in cladodont sharks: with a comparison
901 between primitive grasping and swallowing, and modern cutting and
902 gouging feeding mechanisms. *Journal of Vertebrate Paleontology* **21**,
903 214–226. (doi:10.1671/0272)
- 904 37. Hanke GF. 2008 *Promesacanthus eppleri* n. gen., n. sp., a mesacanthid
905 (Acanthodii, Acanthodiformes) from the Lower Devonian of northern
906 Canada. *Geodiversitas* **30**, 287–302.
- 907 38. Hanke GF, Davis SP. 2008 Redescription of the acanthodian
908 *Gladiobrachus probaton* Bernacsek & Dineley, 1977, and comments on
909 diplacanthid relationships. *Geodiversitas* **30**, 303–330.
- 910 39. Ørvig T. 1967 Some new acanthodian material from the lower Devonian of
911 Europe. *Zool. J. Linn. Soc.* **47**, 131–153.
- 912 40. Zhu M *et al.* 2013 A Silurian placoderm with osteichthyan-like marginal jaw
913 bones. *Nature* **502**, 188–93. (doi:10.1038/nature12617)
- 914 41. Giles S, Friedman M, Brazeau MD. 2015 Osteichthyan-like cranial
915 conditions in an Early Devonian stem gnathostome. *Nature* **520**, 82–175.
916 (doi:10.1038/nature14065)
- 917 42. Chevrinai M, Sire J-Y, Cloutier R. 2017 From body scale ontogeny to
918 species ontogeny: Histological and morphological assessment of the Late
919 Devonian acanthodian *Triazeugacanthus affinis* from Miguasha, Canada.
920 *PLOS ONE* **12**, e0174655. (doi:10.1371/journal.pone.0174655)
- 921 43. King B, Qiao T, Lee MSY, Zhu M, Long JA. 2016 Bayesian Morphological
922 Clock Methods Resurrect Placoderm Monophyly and Reveal Rapid Early
923 Evolution in Jawed Vertebrates. *Syst. Biol.* **66**, 499–516.
924 (doi:10.1093/sysbio/syw107)
- 925 44. Dearden RP, Stockey C, Brazeau MD. 2019 The pharynx of the stem-
926 chondrichthyan *Ptomacanthus* and the early evolution of the gnathostome
927 gill skeleton. *Nat. Commun.* **10**, 1–7. (doi:10.1038/s41467-019-10032-3)
- 928 45. Long JA. 1986 New ischnacanthid acanthodians from the Early Devonian
929 of Australia, with comments on acanthodian interrelationships. *Zool. J.*
930 *Linn. Soc.* **87**, 321–339.
- 931 46. Lindley ID. 2000 Acanthodian fish remains from the Lower Devonian
932 Cavan Bluff Limestone (Murrumbidgee Group), Taemas district, New
933 South Wales. *Alcheringa* **24**, 11–35.
- 934 47. Lindley ID. 2002 Lower Devonian ischnacanthid fish (Gnathostomata:
935 Acanthodii) from the Taemas Limestone, Lake Burrinjuck, New South

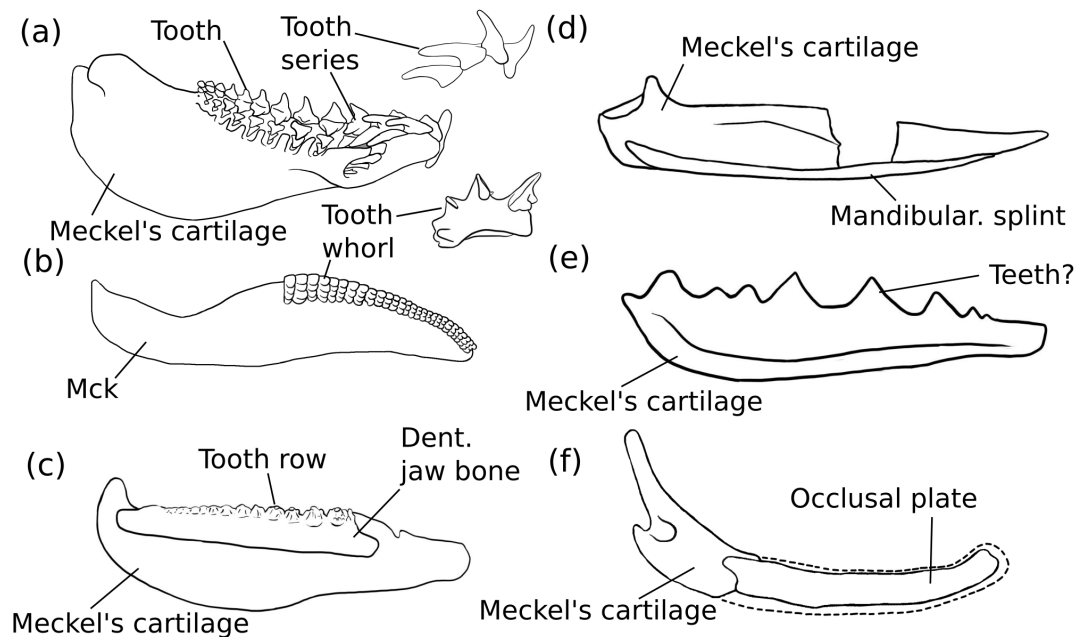
- 936 Wales. *Alcheringa Australas. J. Palaeontol.* **25**, 269–291.
937 (doi:10.1080/03115510108527804)
- 938 48. Burrow CJ. 2004 A Redescription of *Atopacanthus dentatus* Hussakof and
939 Bryant , 1918 (*Acanthodii* , *Ischnacanthidae*). *Jvp* **24**, 257–267.
940 (doi:10.1671/1928)
- 941 49. Hussakof L, Bryant WL. 1918 Catalog of the fossil fishes in the Museum of
942 Buffalo Society of Natural Sciences. *Bull. Buffalo Soc. Nat. Sci.* **12**, 5–178.
- 943 50. Jessen H. 1973 Weitere fischreste aus dem Oberen Plattenkalk der
944 Bergisch-Gladbach Paffrather Mulde (Oberdevon, Rheinisches
945 Schiefergeb.pdf. *Palaeontogr. Abt. A* **1–6**, 159–187.
- 946 51. Denison R. 1979 *Handbook of Palaeoichthyology: Acanthodii*. Verlag Dr.
947 Friedrich Pfeil.
- 948 52. Newman MJ, Burrow CJ, Blaauwen JLD. 2019 A new species of
949 ischnacanthiform acanthodian from the Givetian of Mimerdalen , Svalbard.
950 *Nor. J. Geol.* **99**, 1–13.
- 951 53. Dineley DL, Metcalf S J. 1999 *Fossil Fishes of Great Britain*.
952 Peterborough: Joint Nature Conservation Committee.
- 953 54. Miles RS. 1973 Relationships of acanthodians. In *Interrelationships of*
954 *fishes* (eds P Greenwood, RS Miles, C Patterson), pp. 63–103. London:
955 Zoological Journal of the Linnean Society.
- 956 55. Goloboff PA, Catalano SA. 2016 TNT version 1.5, including a full
957 implementation of phylogenetic morphometrics. *Cladistics* **32**, 221–238.
- 958 56. Gross W. 1971 Downtonische und Dittonische acanthodier-reste des
959 Ostseegebietes. *Palaeontogr. Abt. A* **136**, 1–82.
- 960 57. Miles RS. 1966 The acanthodian fishes of the Devonian Plattenkalk of the
961 Paffrath Trough in the Rhineland with an appendix containing a
962 classification of the *Acanthodii* and a revision of the genus
963 *Homalacanthus*. *Ark. För Zool.* **18**, 147–194.
- 964 58. Blais SA, MacKenzie LA, Wilson MVH. 2011 Tooth-like scales in Early
965 Devonian eugnathostomes and the outside-in hypothesis for the origins of
966 teeth in vertebrates. *J. Vertebr. Paleontol.* **31**, 1189–1199.
967 (doi:10.1080/02724634.2011.607992)
- 968 59. Burrow CJ, Blaauwen JD, Newman M. 2020 A redescription of the three
969 longest-known species of the acanthodian *Cheiracanthus* from the Middle
970 Devonian of Scotland. *Palaeontol. Electron.* **23**, 1–43.
- 971 60. Zidek J. 1985 Growth in *Acanthodes* (*Acanthodii*: Pisces) data and
972 implications. *Palaontologische Z.* **59**, 147–166.

- 973 61. Schultze H-P. 1972 *Homalacanthus*, ein oberdevonischer Acanthodier mit
974 Haifisch-ähnlichen Zähnen. *Neues Jahrb. Für Geol. Paläontol.* , 315–320.
- 975 62. Watson DMS. 1937 The Acanthodian Fishes. *Philos. Trans. R. Soc. Lond.*
976 *B. Biol. Sci.* **228**, 49–146. (doi:10.2307/1436828)
- 977 63. Hanke GF, Wilson MVH. 2004 New teleostome fishes and acanthodian
978 systematics. In *Recent Advances in the Origin and Early Radiation of*
979 *Vertebrates* (eds G Arratia, MVH Wilson), pp. 189–216. München,
980 Germany.
- 981 64. Newman MJ, Burrow CJ, Blaauwen JLD, Davidson RG. 2014 The Early
982 Devonian acanthodian *Euthacanthus macnicoli* Powrie, 1864 from the
983 Midland Valley of Scotland. *Geodiversitas* **36**, 321.
984 (doi:10.5252/g2014n3a1)
- 985 65. Hanke GF, Wilson MVH. 2010 The putative stem-group chondrichthyans
986 *Kathemacanthus* and *Seretolepis* from the Lower Devonian MOTH
987 locality, Mackenzie Mountains, Canada. In *Phylogeny and*
988 *Paleobiogeography of Fossil Fishes* (eds DK Elliott, JG Maisey, X Yu, D
989 Miao), pp. 159–182. München, Germany: Verlag Dr. Friedrich Pfeil.
- 990 66. Smith MM, Coates MI. 1998 Evolutionary origins of the vertebrate
991 dentition: phylogenetic patterns and developmental evolution. *Eur. J. Oral*
992 *Sci.* **106**, 482–500
- 993 67. Burrow CJ, Davidson RG, Den Blaauwen JL, Newman MJ. 2015 Revision
994 of *Climatius reticulatus* Agassiz, 1844 (Acanthodii, Climatidae), from the
995 Lower Devonian of Scotland, based on new histological and morphological
996 data. *J. Vertebr. Paleontol.* **35**, e913421.
997 (doi:10.1080/02724634.2014.913421)
- 998 68. Schultze H, Zidek J. 1982 Ein primitiver acanthodier (pisces) aus dem
999 unterdevon Lettlands. *Paläontologische Z.* **56**, 95–105.
1000 (doi:10.1007/BF02988788)
- 1001 69. Zangerl R. 1981 *Handbook of Paleoichthyology, Chondrichthyes I,*
1002 *Paleozoic Elasmobranchii*. Stuttgart: Gustav Fischer Verlag.
- 1003 70. Valiukevičius J. 1992 First articulated *Poracanthodes* from the Lower
1004 Devonian of Severnaya Zemlya. In *Fossil Fishes as Living Animals*, pp.
1005 193–213.
- 1006 71. Valiukevičius J. 2003 Devonian acanthodians from Severnaya Zemlya
1007 Archipelago (Russia). **25**, 131–204.
- 1008 72. Giles S, Coates MI, Garwood RJ, Brazeau MD, Atwood R, Johanson Z,
1009 Friedman M. 2015 Endoskeletal structure in *Cheirolepis* (Osteichthyes,
1010 Actinopterygii), An early ray-finned fish. *Palaeontology* **58**.
1011 (doi:10.1111/pala.12182)

- 1012 73. Burrow CJ, Rudkin D. 2014 Oldest near-complete acanthodian: The first
1013 vertebrate from the silurian bertie formation Konservat-Lagerstätte,
1014 Ontario. *PLoS ONE* **9**, e104171. (doi:10.1371/journal.pone.0104171)
- 1015 74. Burrow CJ, Young GC. 2012 New Information on *Culmacanthus*
1016 (Acanthodii : Diplacanthiformes) from the ?Early – Middle Devonian of
1017 Southeastern Australia. *Proc. Linn. Soc. New South Wales* **134**, 21–29.
- 1018 75. Hanke GF, Davis SP. 2008 Redescription of the acanthodian
1019 *Gladiobrachus probaton* Bernacsek & Dineley, 1977, and comments on
1020 diplacanthid relationships. *Geodiversitas* **30**, 303–330.
- 1021 76. Young GC, Burrow CJ. 2004 Diplacanthid acanthodians from the Aztec
1022 Siltstone (late Middle Devonian) of southern Victoria Land, Antarctica.
1023 *Foss. Strata* **50**, 23-43
- 1024 77. Gagnier P, Hanke GF, Wilson MVH. 1999 *Tetanopsyrus lindoei* gen. et sp.
1025 nov., an Early Devonian acanthodian from the Northwest Territories,
1026 Canada. *Acta Geol. Pol.* **49**, 81–96.
- 1027 78. Hanke GF, Davis SP. 2008 Redescription of the acanthodian
1028 *Gladiobrachus probaton* Bernacsek & Dineley, 1977, and comments on
1029 diplacanthid relationships. *Geodiversitas* **30**, 303–330.
- 1030 79. Burrow CJ, Trinajstić K, Long JA. 2012 First acanthodian from the Upper
1031 Devonian (Frasnian) Gogo Formation , Western Australia. *Hist. Biol.* **24**,
1032 349–357. (doi:10.1080/08912963.2012.660150)
- 1033 80. Long JA. 1986 A new Late Devonian acanthodian fish from Mt. Howitt,
1034 Victoria, Australia, with remarks on acanthodian biogeography. *Proc. R.*
1035 *Soc. Vic.* **98**, 1–17.
- 1036 81. Grogan ED, Lund R. 2000 *Debeerius ellefseni* (Fam. Nov., Gen. Nov.,
1037 Spec. Nov.), an Autodiastylic Chondrichthyan From the Mississippian Bear
1038 Gulch Limestone of Montana (USA), the Relationships of the
1039 Chondrichthyes, and Comments on Gnathostome Evolution. *Journal of*
1040 *Morphology.* **243**: 219-245.
- 1041 82. Kamminga P, De Bruin PW, Geleijns J, Brazeau MD. 2017 X-ray
1042 computed tomography library of shark anatomy and lower jaw surface
1043 models. *Scientific Data*, 1–6.

1044

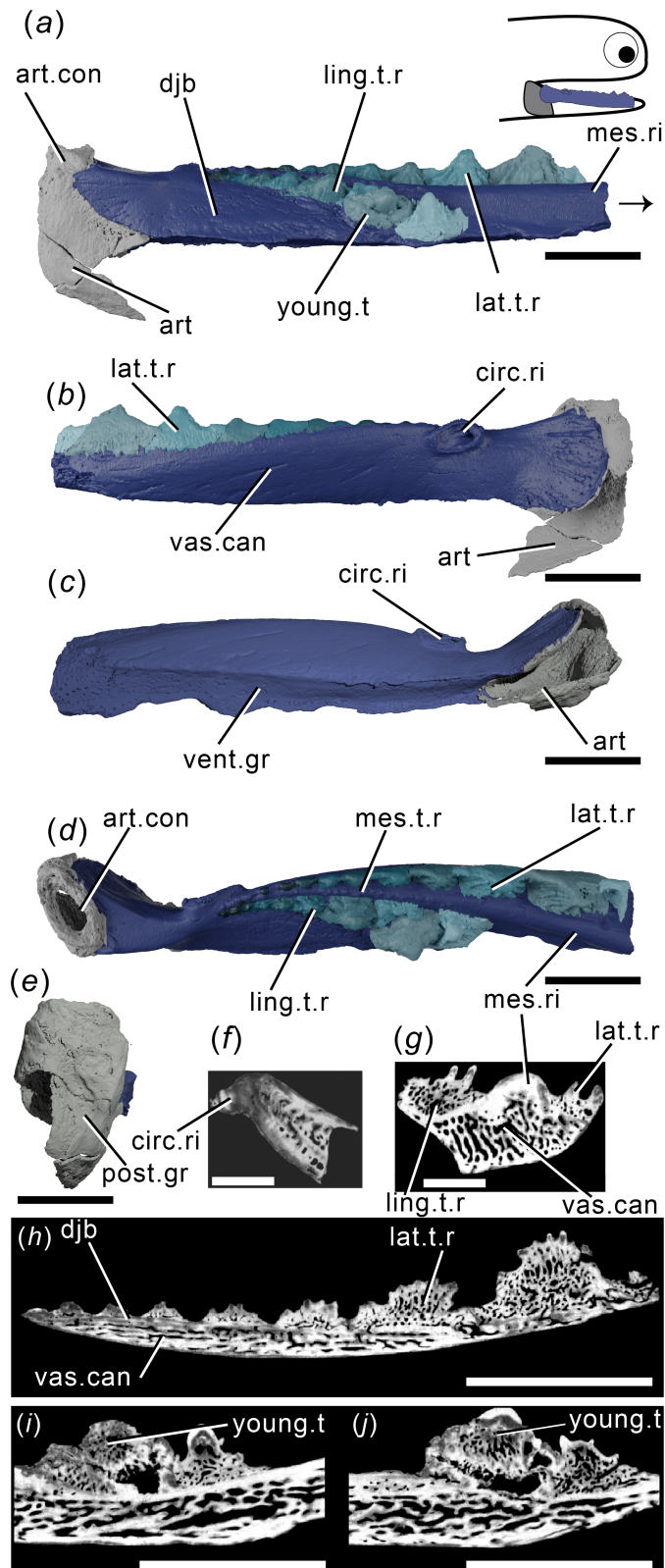
Figure captions



1045

1046 **Figure 1.** Summary figure showing lower jaws of six chondrichthyans, and
1047 major structures discussed in the text. (a) the extant elasmobranch *Isurus* in
1048 medial view and with tooth series in lateral view, drawn from 3D data [82]; (b)
1049 the stem-chondrichthyan *Ptomacanthus* in medial view reconstructed from
1050 [44] and with tooth whorl from [21] (c) the ischnacanthid stem-chondrichthyan
1051 *Erymnacanthus* in medial view redrawn from [25] (d) the acanthodid stem-
1052 chondrichthyan *Acanthodes* in lateral view redrawn from [54] (e) the
1053 ?acanthodid stem-chondrichthyan *Acanthodopsis* in lateral view redrawn from
1054 Burrow [23]; (f) the diplacanthid stem-chondrichthyan *Diplacanthus* in medial
1055 view reconstructed from Watson *et al.*[61] and Burrow *et al.* [28] Not to scale.

1056



1057

1058 **Figure 2.** Tomographic model of the left lower jaw of *Taemasacanthus erroli*

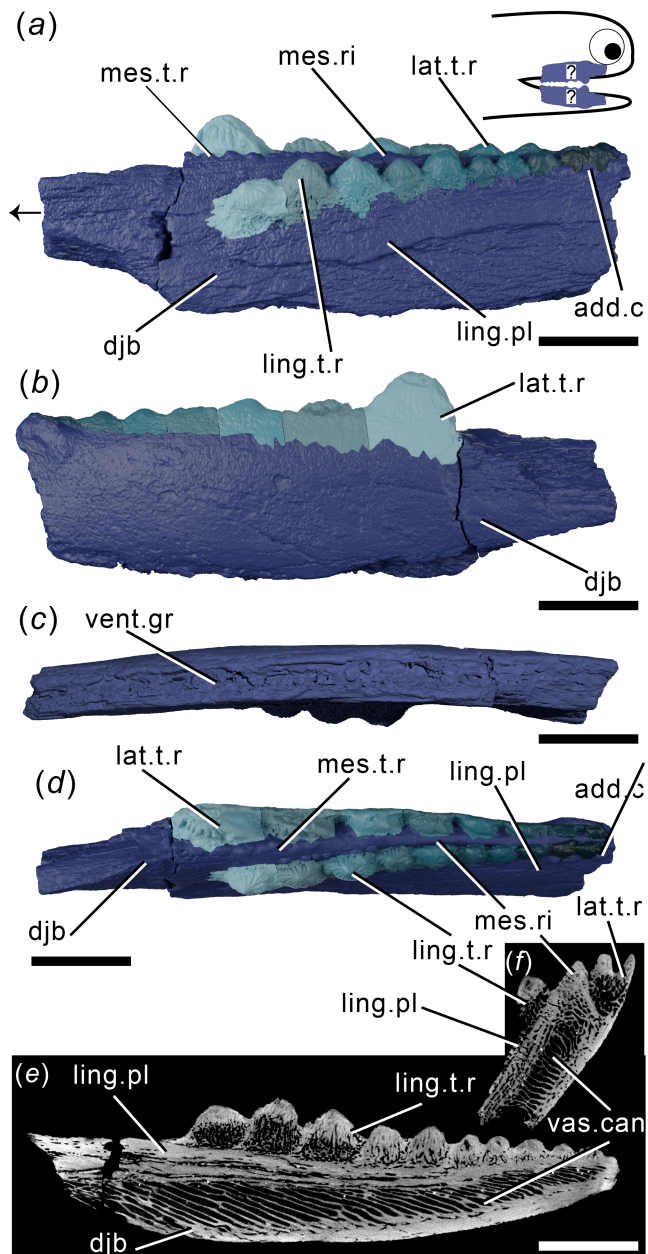
1059 NHMUK PV P.33706 in (a) medial view, (b) lateral view, (c) ventral view, (d)

1060 dorsal view, (e) posterior view, and reconstructed tomograms showing (f) a

1061 transverse section through the circular ridge, (*g*) a transverse section through
1062 the lower jaw, (*h*) a sagittal section through the lingual tooth row and (*i*)-(*j*)
1063 progressively medial sagittal sections through the aberrant youngest cusp and
1064 neighbouring cusps. Teeth in panels (*a*), (*b*) and (*d*) are coloured separately
1065 from the dentigerous jaw bone. Arrow indicates direction of anterior, and top
1066 right inset shows location of rendered jaw components. Abbreviations: art,
1067 articular (Meckel's cartilage); art.con, articular 'condyle'; circ.ri, circular ridge;
1068 djb, dentigerous jaw bone; lat.t.r., lateral tooth row; ling.t.r, lingual tooth row;
1069 mes.ri, mesial ridge; mes.t.r, mesial tooth row; post.gr, posterior groove;
1070 young.t, out-of-order youngest tooth; vent.gr, ventral groove; vas.can,
1071 vascular canals. Scale bar = 5 mm.

1072

1073



1074

1075 **Figure 3.** Tomographic model of a dentigerous jaw bone of *Atopacanthus* sp.

1076 NHMUK PV P.10978 in (a) medial view, (b) lateral view, (c) ventral view, (d)

1077 dorsal view and (e) a reconstructed tomogram showing a sagittal section

1078 through the lingual tooth row. Arrow indicates direction of anterior, and top

1079 right inset shows possible locations of rendered jaw components. Teeth in

1080 panels (a), (b) and (d) are coloured separately from the dentigerous jaw bone.

1081 Abbreviations: add.c, additional cusps; djb, dentigerous jaw bone; lat.t.r.,

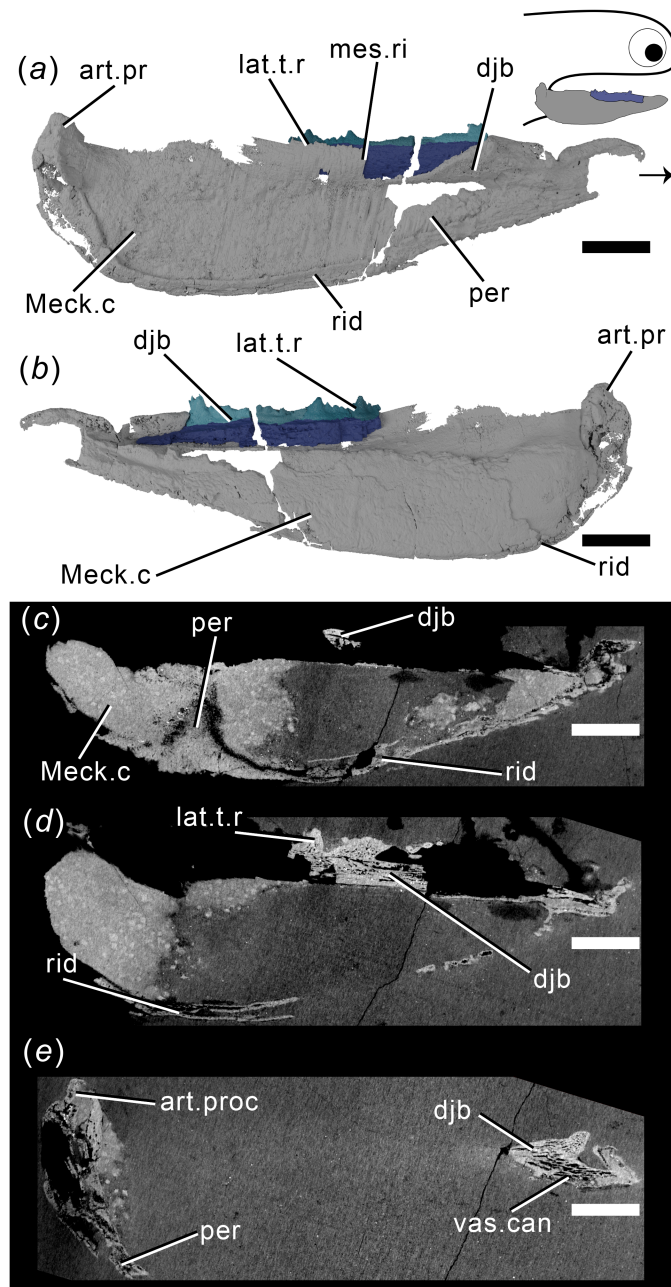
1082 lateral tooth row; ling.pl, lingual plate; ling.t.r, lingual tooth row; mes.ri, mesial

1083 ridge; mes.t.r, mesial tooth row; vent.gr, ventral groove; vas.can, vascular

1084 canals. Scale bar = 5 mm in (a)-(e) and (h)-(j), 2 mm in (f)-(h).

1085

1086



1087

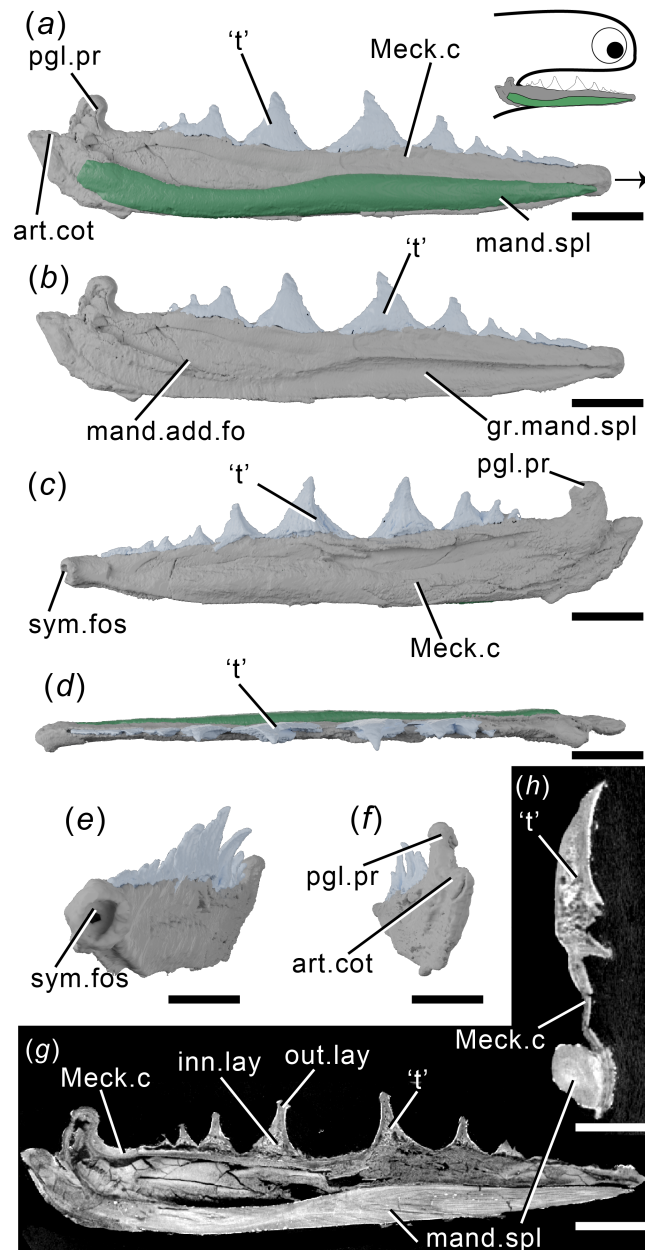
1088 **Figure 4.** Tomographic model of the left lower jaw of *Ischnacanthus* sp.
1089 NHMUK PV P.40124 in (a) lateral view, (b) medial view, and (c), (d), (e)
1090 reconstructed tomograms showing successively deeper sagittal sections.
1091 Arrow indicates direction of anterior, and top right inset shows location of
1092 rendered jaw components. Abbreviations: art.proc, articular process; djb
1093 dentigerous jaw bone; lat.t.r., lateral tooth row; Meck.c, Meckel's cartilage;

1094 mes.ri, mesial ridge; per, perichondral bone; rid, ridge; vas.can, vascular

1095 canal. Scale bar = 5 mm.

1096

1097



1098

1099 **Figure 5.** Tomographic model of the right lower jaw of *Acanthodopsis* sp.

1100 NHMUK PV P.10383 in lateral view with (a) and without (b) mandibular splint,

1101 (c) medial view, (d) dorsal view, (e) anteromedial view, (f) posterior view, and

1102 reconstructed tomograms showing (g) a sagittal section through the entire jaw

1103 and (h) a transverse section through the jaw. Arrow indicates direction of

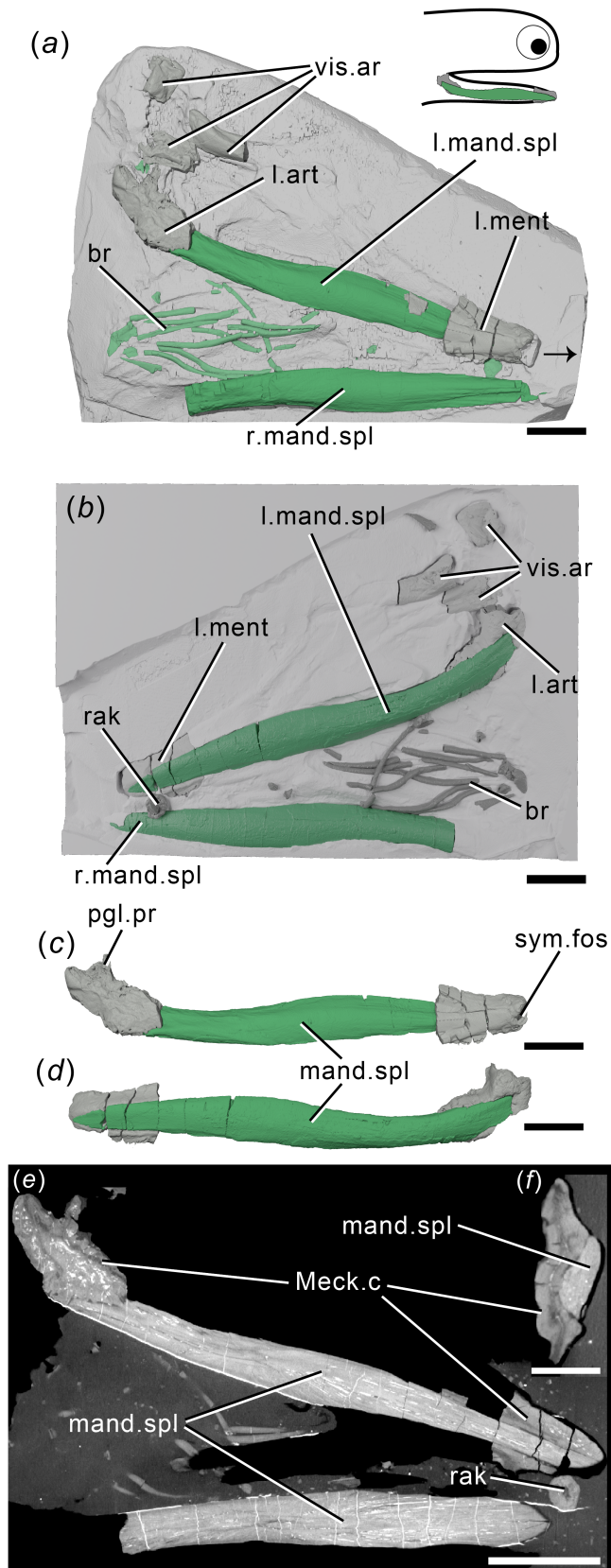
1104 anterior, and top right inset shows location of rendered jaw components.

1105 Abbreviations: art.cot, articular cotylus; gr.mand.spl, groove for mandibular

1106 splint; inn.lay, inner layer; mand.add.fo, mandibular adductor fossa; mand.spl,
1107 mandibular splint; Meck.c, Meckel's cartilage; out.lay, outer layer; pgl.pr,
1108 preglenoid process; sym.fos, symphyseal fossa; 't', 'teeth'. Scale bar = 5 mm
1109 in (a)-(g), 2 mm in (h).

1110

1111



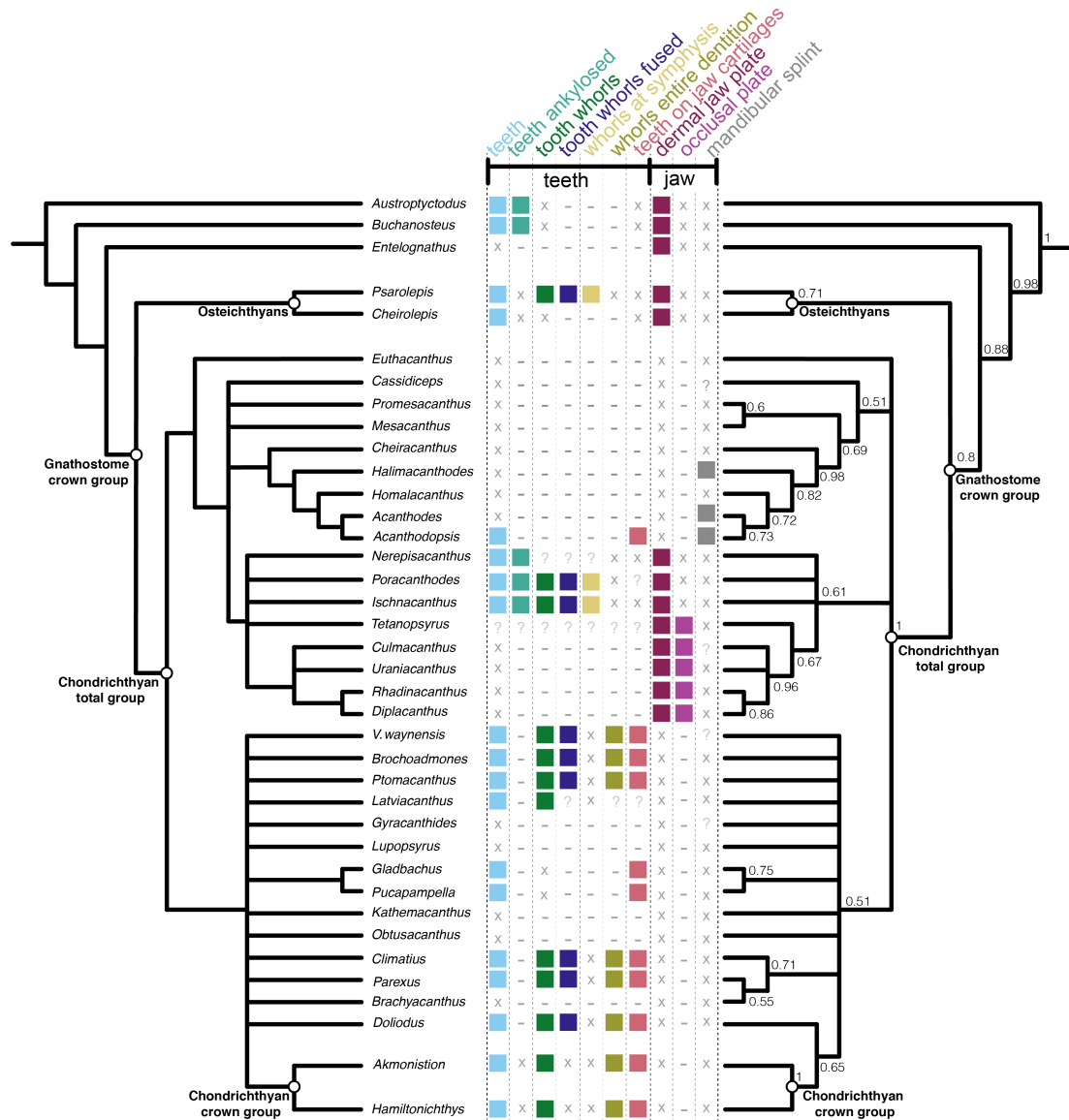
1112

1113 **Figure 6.** The lower jaws of *Acanthodes* sp. NHMUK PV P.8065 in (a) dorsal

1114 view against the matrix, (b) in ventral view superimposed on a digital mould of

1115 the matrix's surface, the left lower jaw isolated in (c) medial and (d) lateral
1116 view, and reconstructed tomograms showing (e) a coronal section through the
1117 specimen, and (f) a transverse section through a lower jaw. Arrow indicates
1118 direction of anterior, and top right inset shows location of rendered jaw
1119 components. Abbreviations: art, articular (Meckel's cartilage); br,
1120 branchiostegal rays; mand.spl, mandibular splint; Meck.c, Meckel's cartilage;
1121 ment, mentomandibular (Meckel's cartilage); pgl.pr, preglenoid process; rak,
1122 gill raker; sym.fos, symphyseal fossa; vis.ar, visceral arch fragments. Scale
1123 bar = 5 mm in (a)-(e), 2mm in (f).

1124



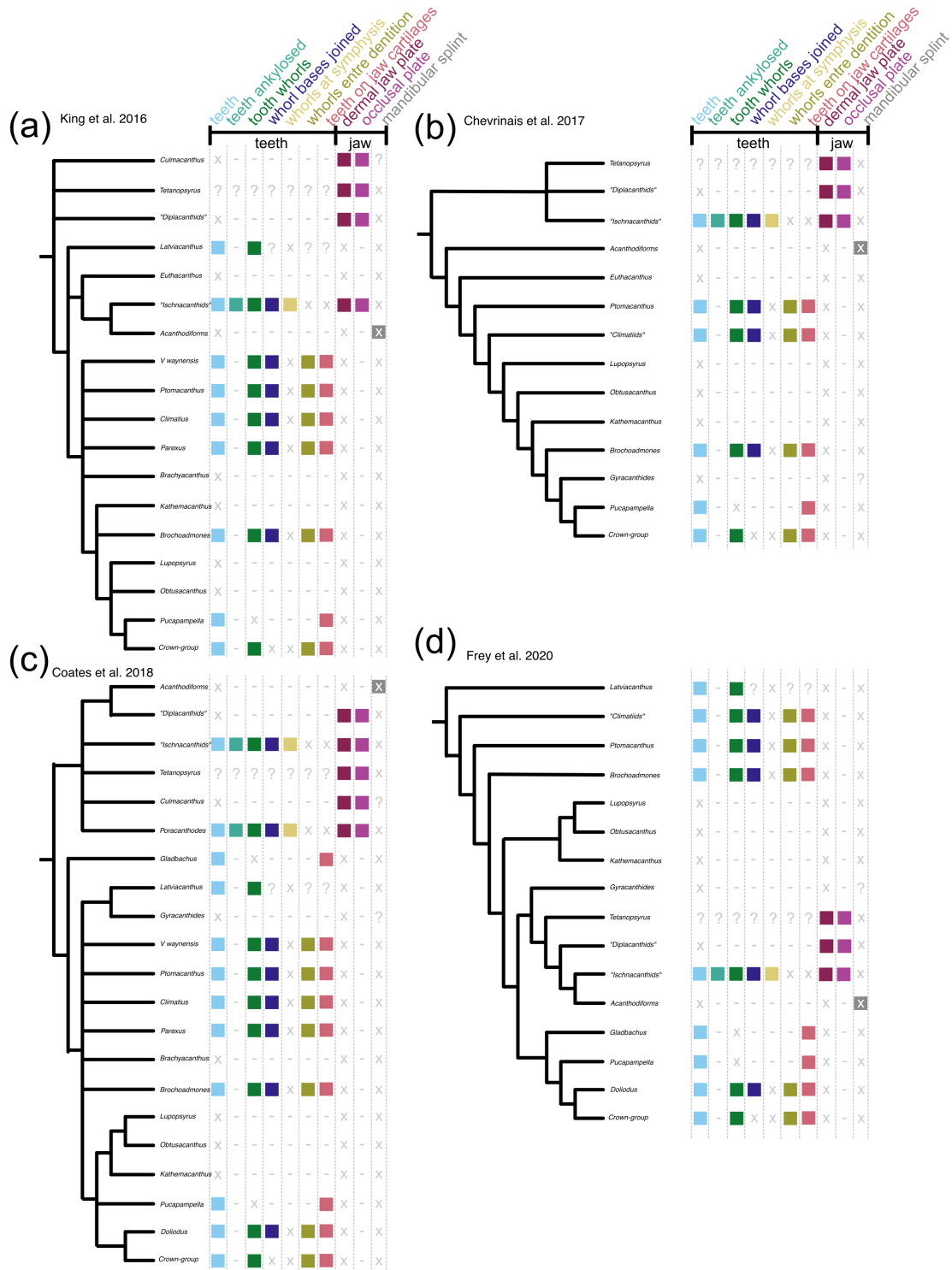
1125

1126 **Figure 7.** Phylogenetic relationships of early chondrichthyans and distribution
 1127 of oral structures. Strict consensus of 26101 most parsimonious trees on left
 1128 and Bayesian analysis on right, with some non-chondrichthyan taxa excluded
 1129 (full tree with support values in figures S2 and S3). Numbers at nodes on right
 1130 represent Bayesian posterior probabilities. Character distribution is based on
 1131 coding in the data matrix as follows: teeth, character (c.) 82; teeth ankylosed,
 1132 c.93; tooth whorls fused, c. 85; whorls at symphysis and whorls entire
 1133 dentition, c.88; teeth on jaw cartilages and dermal jaw plate, c.94 ; occlusal
 1134 plate, c.269 ; mandibular splint, c.268. Filled boxes indicate presence of

1135 feature; 'x' indicates feature absent; '?' indicates uncertainty; '-' indicates

1136 inapplicability.

1137



1138

1139 **Figure 8.** Summaries of four contrasting recent phylogenetic schemes of early

1140 chondrichthyans, with distribution of oral characters. (a) King *et al.* 2016 [43],

1141 (b) Chevrainais *et al.* 2017 [42], (c) Coates *et al.* 2018 [24], (d) Frey *et al.* 2020

1142 [35]. Icons and character numbers as in Fig. 7 Acanthodiforms includes taxa
1143 both with and without mandibular splints.

1144

1145 **Supplementary material (separate pdf)**

1146 Supplementary information for this manuscript is included as two files. The
1147 first includes notes on the phylogenetic analysis (taxon addition, character
1148 addition and coding changes) supplementary table 1, and supplementary
1149 figures 1-3. The second is a zipped folder containing all files necessary for
1150 replicating our Bayesian and parsimony analyses.

1151